Joint Transmit Resource Management and Waveform Selection Strategy for Target Tracking in Distributed Phased Array Radar Network

Chenguang Shi, *Member, IEEE,* Yijie Wang, Sana Salous, *Senior Member, IEEE,* Jianjiang Zhou, *Member, IEEE,* and Junkun Yan, *Senior Member, IEEE*

***Abstract*—In this paper, a joint transmit resource management and waveform selection (JTRMWS) strategy is put forward for target tracking in distributed phased array radar network. We establish the problem of joint transmit resource and waveform optimization as a dual-objective optimization model. The key idea of the proposed JTRMWS scheme is to utilize the optimization technique to collaboratively coordinate the transmit power, dwell time, waveform bandwidth, and pulse length of each radar node in order to improve the target tracking accuracy and low probability of intercept (LPI) performance of distributed phased array radar network, subject to the illumination resource budgets and waveform library limitation. The analytical expressions for the predicted Bayesian Cramér-Rao lower bound (BCRLB) and the probability of intercept are calculated and subsequently adopted as the metric functions to evaluate the target tracking accuracy and LPI performance, respectively. It is shown that the JTRMWS problem is a non-linear and non-convex optimization problem, where the above four adaptable parameters are all coupled in the objective functions and constraints. Combined with the particle swarm optimization (PSO) algorithm, an efficient and fast three-stage-based solution technique is developed to deal with the resulting problem. Simulation results are provided to verify the effectiveness and superiority of the proposed JTRMWS algorithm compared with other state-of-the-art benchmarks.**

***Index Terms*—Joint transmit resource management and waveform selection (JTRMWS), Bayesian Cramér-Rao lower bound (BCRLB), low probability of intercept (LPI), target tracking, distributed phased array radar network.**

I. Introduction

A. Background and Literature Review

In recent years, the concept of transmit resource-aware management is of vital importance for target tracking application in distributed phased array radar network and has been extensively studied from various aspects to enhance resource usage efficiency, where there exists a contradiction between target tracking accuracy demand and illumination resource consumption in radar system [1]-[3]. Technically speaking, the resource-aware management and scheduling strategy for target tracking can be described as an optimization model to find a trade-off between the target tracking performance and finite system resource.

In general, there are series of resource-aware management schemes for radar systems concentrating on achieving much better resource usage efficiency [4]-[6], which can be divided into two categories. The first one is designed to maximize the target tracking performance for certain system resource budgets. For instance, the authors in [7] investigate the problem of joint node selection and power allocation for multi-target tracking in decentralized radar networks, whose purpose is to minimize the worst-case tracking predicted conditional Cramér-Rao lower bound (PC-CRLB) with multiple targets. A two-step semi-definite programming-based solution approach is presented to solve the resulting problem. In [8], Sun et al. concentrate on the problem of joint power and bandwidth allocation for target tracking in clutter with an asynchronous radar network system, and the branch-reduce-and-bound technique is adopted to deal with the non-convex optimization model. It is validated that the target state estimation error can be efficiently decreased with the optimized illumination resource allocation. Later, the work of [9] extends the above study to netted colocated multiple-input multiple-output (MIMO) radar case in order to achieve better target position estimation accuracy subject to certain system resource constraints. In [10], a joint subarray selection and power allocation scheme for multiple targets tracking employing large-scale MIMO radar networks is developed, which aims to enhance the overall target tracking performance by cooperatively adjusting transmitter selection, receiver selection, and power allocation. It is also illustrated that the relative geometry, target radar cross section (RCS), and weight coefficients affect the resource allocation results. In [11], a robust power allocation algorithm is proposed for resource-aware multi-target tracking in colocated MIMO radar, where a task utility function is defined and utilized to assess the target tracking accuracy for various power allocation strategies in a flexible behavior. The iterative parallel search technique is exploited to attain the solutions. More recently, in [12], a target capacity-based resource optimization algorithm in radar networks is proposed for target

This work was supported in part by the National Natural Science Foundation of China under Grant 61801212, in part by the Key Laboratory of Equipment Pre-Research Foundation under Grant 6142401200402, in part by the Natural Science Foundation of Jiangsu Province under Grant BK20180423, in part by the National Aerospace Science Foundation of China under Grant 20200020052002 and Grant 20200020052005, in part by National Defense Science and Technology Innovation Special Zones, and in part by Key Laboratory of Radar Imaging and Microwave Photonics (Nanjing Univ. Aeronaut. Astronaut.), Ministry of Education, Nanjing, China. (*Corresponding author: Chenguang Shi*)

C. G. Shi, Y. J. Wang, F. Wang, and J. J. Zhou are with Key Laboratory of Radar Imaging and Microwave Photonics (Nanjing University of Aeronautics and Astronautics), Ministry of Education, Nanjing University of Aeronautics and Astronautics, Nanjing 210016, China.

S. Salous is with School of Engineering and Computing Sciences, Durham University, Durham, DH1 3LE, U.K..

Junkun Yan is with National Laboratory of Radar Signal Processing, Xidian University, Xi'an, China.

tracking application. The primary objective of the optimization model is maximize the number of targets that can be tracked with given accuracy requirements by coordinating the transmit power and dwell time of different radars. It is worth to point out that the value of false alarm rate has great impact on the target tracking performance in radar systems. However, in aforementioned resource-aware management studies, the false alarm rate selection and power allocation frameworks are separately discussed. Reference [13] puts forth a collaborative detection and power allocation strategy for target tracking in multiple radars configuration, which optimizes the false alarm rate and transmit power of each radar node under the constraints of some resource budgets.

The latter item is to minimize the system resource consumption for predetermined target tracking performance demands. In practice, the available transmit resources in different radar systems are usually limited. On the other side, the low probability of intercept (LPI) issue is a crucial and essential demand of military applications in modern battlefield [14]-[18]. Reference [19] builds the relationship between radar resource and target tracking accuracy, and analyzes how the sampling interval, transmit power, and waveform parameters influence the tracking filter in clutter. In [20], the authors apply the idea of LPI-based joint transmitter selection and resource management for target tracking in radar networks, aiming at minimizing the probability of intercept by collaboratively controlling the revisit interval, dwell time, illumination power, and transmitter selection for predefined target tracking performance. Reference [21] investigates the power minimization-based robust orthogonal frequency division multiplexing (OFDM) radar waveform design criteria to guarantee the specified mutual information threshold for target state estimation. The authors in [22] formulate a cooperative node and waveform allocation approach for multiple targets tracking in distributed radar network, which intends to optimize the selection of radar nodes with corresponding waveforms to achieve a certain tracking demand at the lowest resource burden. The study in [23] develops a joint waveform selection and time-space resource management method for colocated MIMO radar system, where the sampling period, the designated radars, the target-radar assignment, the subarray number, the transmit energy, and the waveform parameters of each activated radar are adaptively coordinated to minimize the tracking errors of multiple targets and the overall system resource consumption in the meantime.

On the basis of the aforementioned literature, the existing studies have made seminal contributions to the field of transmit resource scheduling in cognitive radar systems. Nevertheless, in some specific application backgrounds, those resource management strategies cannot be put into use straightway. Additionally, there are still some problems on resource-aware management in distributed radar network to be highlighted. Firstly, in theory, maximization of the target tracking accuracy and minimization of the illumination resource consumption are two conflicting goals, which are of importance and should be taken into consideration simultaneously. Secondly, although the transmit resources and waveform parameters have influence on the target tracking performance, they are separately discussed in previous strategies [2]-[13]. Practically, in order to achieve better target tracking performance, it is advantageous for us to integrate the resource-aware management and waveform selection schemes into a coherent framework. To this end, we need to establish appropriate evaluation mechanisms for target tracking performance and LPI performance respectively, formulate suitable objective functions in view of system resource constraints, and subsequently develop efficient and fast solution methodology to tackle the underlying optimization problem. Then, the distributed phased array radar network is capable of adjusting its resource allocation and waveform selection to track the target effectively. To realize this, a joint transmit resource management and waveform selection (JTRMWS) scheme is proposed for target tracking in distributed phased array radar network, with the aim of improving the target tracking accuracy and LPI performance at the same time while meeting several resource budgets and waveform library limitation. To the best of our knowledge, there has been no such JTRMWS scheme for target tracking application in distributed phased array radar network until now. This gap motivates this work.

B. Major Contributions

The main contributions of this article can be summed up as follows:

- *The analytical expressions for the predicted Bayesian Cramér-Rao lower bound (BCRLB) and the probability of intercept are derived, which are employed to evaluate the target tracking accuracy and LPI performance of radar network, respectively.*
- *By integrating the resource-aware management and waveform selection frameworks into a coherent one, a JTRMWS scheme is put forward for target tracking in distributed phased array radar network, which is subsequently described as a non-linear and non-convex optimization problem.* Previously, the transmit resource management and waveform selection strategies are always addressed separately, and the relationships between them are ignored. However, both the illumination resources and waveform parameters have impacts on the target tracking accuracy. Mathematically speaking, the JTRMWS strategy aims to simultaneously minimize the predicted BCRLB and the probability of intercept of the underlying system subject to the constraints of transmit resource budgets and waveform library, through adjusting the transmit power, dwell time, waveform bandwidth, and pulse length of each radar.
- *In order to solve the resulting non-linear and non-convex optimization problem in real time, we develop an efficient and fast three-stage-based solution methodology incorporating particle swarm optimization (PSO) approach.* It is quite difficult to deal with a non-linear and non-convex optimization problem, and thus we propose the following three-step solution technique to obtain the feasible solutions. In Stage (1), by employing appropriate relaxation reformulation and problem partition, the original optimization problem is equivalently recast as

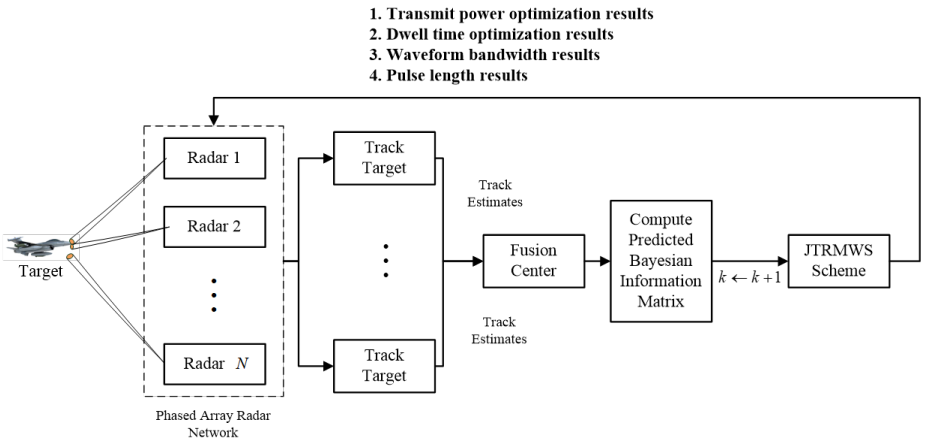

Fig. 1. The sketch map of the closed-loop JTRMWS procedure.

two sub-problems. In Stage (2), we strictly prove that the probability of intercept of each radar node is an upper convex function with respect to its dwell time, and the optimal value of dwell time can be obtained at the boundary. Then, the obtained dwell time results are utilized to calculate the transmit power of multiple radars. In Stage (3), to accelerate the solution process and to guarantee the real-time demand, the particle swarm optimization (PSO) algorithm is exploited to find the reasonable feasible waveform bandwidth and pulse length in the given waveform library.

- *A closed-loop JTRMWS procedure for target tracking in a phased array radar network is built.* Owing to the non-linearity of the measurement model, we use the interacting multiple model-extended Kalman filtering (IMM-EKF) method to obtain the target state estimates. Then, the value of BCRLB is computed for the next tracking instant based on the predicted target state for the next optimization period. Subsequently, the JTRMWS optimization problem is formulated and solved using the developed efficient solution methodology. In the end, the optimization results are sent back to each radar node to guide probing strategy for the next tracking instant to maximize the LPI and target tracking performance. The sketch map of the JTRMWS strategy for target tracking is depicted in Fig. 1.
- *Extensive numerical results are provided to validate the effectiveness and superiority of our proposed JTRMWS scheme, in terms of the achievable target tracking accuracy and LPI performance of the distributed phased array radar network.* To be more specific, the presented JTRMWS scheme is able to achieve better trade-off between target tracking accuracy and LPI performance with much lower operation time consumption when compared to other benchmarks, demonstrating the advantages of the proposed strategy. Particularly, it is demonstrated that the proposed three-stage-based solution technique can offer close performance to the exhaustive search-based method. In addition, it is also shown that the JTRMWS results are affected by the configuration of the phased array radar network with respect to the target and the target reflectivity.

C. Organization of the Paper

The rest of the current study is structured as follows: Section II introduces the signal model and system model. The JTRMWS strategy is presented in Section III. The basis of the proposed strategy is introduced in Section III-A. In Sections III-B and III-C, the analytical expressions for the predicted BCRLB and the probability of intercept are introduced and utilized as performance metrics to characterize the target tracking accuracy and LPI performance, respectively. The mathematical optimization model for the JTRMWS strategy is built and resolved by employing a developed efficient three-stage-based solution technique in Sections III-D and III-E, respectively. Numerical simulations are provided in Section IV to demonstrate the advantages of the proposed JTRMWS algorithm. Finally, the concluding remarks of the paper are made in Section V.

II. Signal and System Models

A. Signal Model

Let us consider a distributed phased array radar network, which is composed of N spatially diverse phased array radar nodes. The location of the n-th radar node is denoted as $[x_n, y_n]$. On the other hand, the state of the target at each tracking instant k is $\mathbf{X}_k = [x_k, y_k, \dot{x}_k, \dot{y}_k]^T$, where $[x_k, y_k]$ denotes the target position at the k-th instant, and $[\dot{x}_k, \dot{y}_k]$ denotes the target velocity at the k-th instant. The radar network aims to track the target and has available estimates of some unknown target parameters, such as the target range, Doppler shift, and angle of arrival [24].

To begin with, for the sake of simplicity, the following moderate assumptions are made.

- The transmit waveform of each radar is a narrow-band signal.
- The radar n is equipped with only a matched filter that correlates to its own emitted waveform.

- The time compression due to the Doppler shift can be ignored.
- The hostile passive intercept receiver is mounted on the moving target with an omni-directional antenna.

For the n-th radar node, the transmit signal at the k-th tracking instant is written as:

$$s_{n,k}(t) = \sqrt{P_{n,k}}\tilde{S}_{n,k}(t)\, e^{-j2\pi f_c t}, \tag{1}$$

where f_c denotes the carrier frequency, and $P_{n,k}$ denotes the transmit power of the n-th radar node at instant k. The term $\tilde{S}_{n,k}(t)$ represents the normalized complex envelope of the transmit signal with unit power. For the linear frequency modulation (LFM) signal with a complex Gaussian envelope, the term $\tilde{S}_{n,k}(t)$ can be expressed by:

$$\tilde{S}_{n,k}(t) = \left(\frac{1}{\pi\lambda_{n,k}^2}\right)^{\frac{1}{4}} \exp\left[-\left(\frac{1}{2\lambda_{n,k}^2} - j2\pi b_{n,k}\right)t^2\right], \tag{2}$$

where $b_{n,k}$ represents the frequency modulation rate of radar n at instant k, $b_{n,k} = W_{n,k}/2T_{s,n,k}$, $W_{n,k}$ represents the bandwidth of the transmit waveform at instant k, $T_{s,n,k}$ denotes the effective pulse length, and $\lambda_{n,k}$ denotes the Gaussian pulse length parameter at instant k. The effective pulse length $T_{s,n,k}$ is approximately equal to $7.4338\lambda_{n,k}$, that is, $T_{s,n,k} = 7.4338\lambda_{n,k}$ [25][26].

The received signal at the n-th radar node can be given by:

$$\tilde{r}_{n,k}(t) = s_{n,k}(t-\tau_{n,k})\, e^{-j2\pi v_{n,k}t} + \tilde{n}_{n,k}(t), \tag{3}$$

where $\tilde{n}_{n,k}(t)$ is the additive zero-mean complex white Gaussian noise. $\tau_{n,k}$ and $v_{n,k}$ denote the target time delay and Doppler shift with respect to the n-th radar node at tracking instant k, respectively.

B. Target Dynamic Model

Consider a single target tracking scenario, the target motion can be prescribed by the following two models, i.e., one constant-velocity (CV) model and one coordinated turning (CT) models with two different inverse rotation factors [26]. Therefore, the target dynamic model can be expressed by:

$$\mathbf{X}_k = \mathbf{F}\mathbf{X}_{k-1} + \mathbf{W}_{k-1}, \tag{4}$$

where $\mathbf{F}$ represents the target state transition matrix. For the CV model, the target state transition matrix $\mathbf{F}_{\text{CV}}$ is given by:

$$\mathbf{F}_{\text{CV}} = \begin{bmatrix} 1 & 0 & \Delta T & 0 \\ 0 & 1 & 0 & \Delta T \\ 0 & 0 & 1 & 0 \\ 0 & 0 & 0 & 1 \end{bmatrix}, \tag{5}$$

where ΔT is the revisit interval between successive instants. While for the CT model, the target state transition matrix $\mathbf{F}_{\text{CT}}$ is as follows:

$$\mathbf{F}_{\text{CT}} = \begin{bmatrix} 1 & \frac{\sin(\omega\Delta T)}{\omega} & 0 & \frac{\cos(\omega\Delta T)-1}{\omega} \\ 0 & \cos(\omega\Delta T) & 0 & -\sin(\omega\Delta T) \\ 0 & \frac{1-\cos(\omega\Delta T)}{\omega} & 1 & \frac{\sin(\omega\Delta T)}{\omega} \\ 0 & \sin(\omega\Delta T) & 0 & \cos(\omega\Delta T) \end{bmatrix}, \tag{6}$$

where ω is the angular speed of turning. The term $\mathbf{W}_{k-1}$ in Equation (4) represents the zero-mean Gaussian process noise with a known covariance matrix $\mathbf{Q}_{k-1}$ as follows:

$$\mathbf{Q}_{k-1} = \xi\mathbf{I}_2 \otimes \begin{bmatrix} \frac{(\Delta T_0)^3}{3} & \frac{(\Delta T_0)^2}{2} \\ \frac{(\Delta T_0)^2}{2} & \Delta T_0 \end{bmatrix}, \tag{7}$$

where ξ represents the intensity level of process noise, and $\otimes$ represents the Kronecker product operator.

C. Measurement Model

The measurements $\mathbf{Z}_k$ from multiple radar nodes at tracking instant k have the form $\mathbf{Z}_k = [\mathbf{Z}_{1,k}^T, \cdots, \mathbf{Z}_{n,k}^T, \cdots, \mathbf{Z}_{N,k}^T]^T$, where the measurement obtained by the n-th radar $\mathbf{Z}_{N,k}$ is given by [27][28]:

$$\mathbf{Z}_{n,k} = \mathbf{h}_{n,k}(\mathbf{X}_k) + \mathbf{N}_{n,k}, \tag{8}$$

with

$$\mathbf{h}_{n,k}(\mathbf{X}_k) = [R_{n,k}, v_{n,k}, \theta_{n,k}]^T, \tag{9}$$

where $(\cdot)^T$ is the transpose operator, $R_{n,k}$, $v_{n,k}$, and $\theta_{n,k}$ denote the range, velocity, and angle of arrival measurement components at the n-th radar, respectively. $\mathbf{h}(\mathbf{X}_k)$ denotes the measurement function, $\mathbf{N}_{n,k}$ denotes the measurement error matrix at instant k with covariance $\mathbf{\Psi}_{n,k}$. Thus, the dimension of the measurement is three, with

$$\begin{cases} R_{n,k} = \sqrt{(x_k - x_n)^2 + (y_k - y_n)^2}, \\ v_{n,k} = \frac{\dot{x}_k(x_k - x_n) + \dot{y}_k(y_k - y_n)}{\sqrt{(x_k - x_n)^2 + (y_k - y_n)^2}}, \\ \theta_{n,k} = \arctan(\frac{y_k - y_n}{x_k - x_n}). \end{cases} \tag{10}$$

It is worth pointing out that the measurement error covariance $\mathbf{\Psi}_{n,k}$ is characterized by the waveform parameters, which can be calculated by [26]:

$$\mathbf{\Psi}_{n,k} = \mathbf{T}\mathbf{C}_{n,k}\mathbf{T}, \tag{11}$$

where $\mathbf{T} = \text{diag}[\text{c}/2, \text{c}/(2f_c), 1]$ is the transform matrix from time and Doppler shift to range and range rate, c is the speed of light, $\mathbf{C}_{n,k}$ is the Cramér-Rao lower bound (CRLB) matrix for the radar estimates at radar n. For the Gaussian-LFM signal, $\mathbf{C}_{n,k}$ can further be expressed by [26]:

$$\mathbf{C}_{n,k} = \frac{1}{\text{SNR}_{n,k}} \begin{bmatrix} 2\lambda_{n,k}^2 & -4b_k\lambda_{n,k}^2 & 0 \\ -4b_{n,k}\lambda_{n,k}^2 & \frac{1}{2\pi^2\lambda_{n,k}^2} + 8b^2\lambda_{n,k}^2 & 0 \\ 0 & 0 & \sigma_\theta^2 \end{bmatrix}, \tag{12}$$

where the achieved signal to noise ratio (SNR) $\text{SNR}_{n,k}$ at the n-th radar for the tracking instant k can be calculated by:

$$\text{SNR}_{n,k} = \frac{P_{t,n,k}T_{d,n,k}G_{t,n}G_{r,n}\sigma_n\lambda_t^2 G_{\text{RP}}}{(4\pi)^3 T_r R_{n,k}^4 k_0 T_0 B_r F_r}, \tag{13}$$

where $P_{t,n,k}$ is the transmit power of radar n at instant k, $T_{d,n,k}$ is the corresponding dwell time, σ_n is the RCS of target with respect to radar n, $G_{t,n}$ is the gain of transmitting antenna at the n-th radar, $G_{r,n}$ is the gain of receiving antenna at the n-th radar, G_{RP} is the processing gain of each radar, T_r is the pulse repetition rate, F_r denotes the noise coefficient of each radar receiver, k_0 denotes Boltzmann constant, T_0 denotes

the noise temperature of each radar receiver, B_{r} denotes the bandwidth of each radar receiver, λ_{t} denotes the signal wavelength, and $R_{n,k}$ represents the range from the target to the n-th radar at instant k. It should be noticed that $\mathrm{SNR}_{n,k}$ is a function of the transmit power $P_{\mathrm{t},n,k}$ and the dwell time $T_{\mathrm{d},n,k}$, which does not depend on the waveform parameters $W_{n,k}$ and $\lambda_{n,k}$.

Remark 1: In the distributed phased array radar network, the multiple radar nodes are deployed far away from one another, which probe the target from various aspect angles [7]. Thus, the measurements from different radars are independent with each other, which are collected and processed comprehensively in the fusion center, leading to a integrated and organic system. In this way, the phased array radar network can offer a large number of benefits over conventional radar nodes that work independently, such as improved probability of detection, better target tracking accuracy, increased area coverage, and so forth.

III. JTRMWS Strategy

A. Basis of the Technique

Mathematically speaking, the proposed JTRWO strategy can be formulated as a dual-objective optimization problem subject to several system constraints. The BCRLB is used as the metric for target tracking accuracy, which bounds the error variance of the unbiased estimates of the unknown target state, while the probability of intercept can be employed to assess the LPI performance of the distributed phased array radar network. The parameters of interest considered here are the transmit power, dwell time, waveform bandwidth, and pulse length of each radar. We are then in a position to optimize the above parameters in order to achieve better target tracking accuracy and LPI performance for the underlying system.

The detailed steps of the JTRMWS scheme are provided as follows.

B. Performance Metric for Target Tracking Accuracy

Since the BCRLB is able to bound the error variance of the target state estimation, and it is predictive at one step ahead in the tracking recursion cycle, we adopt the predicted BCRLB here as a performance metric to quantify the target tracking performance for the JTRMWS scheme. Besides, it is also assumed that the measurements obtained from different radar nodes are independent of one another [27]-[31]. Thus, the predicted Bayesian information matrix (BIM) can be expressed by:

$$\begin{aligned}&\mathbf{J}(\mathbf{X}_{k|k-1},\mathbf{P}_{\mathrm{t},k},\mathbf{T}_{\mathrm{d},k},\mathbf{W}_k,\boldsymbol{\lambda}_k)\\&=\mathbf{J}_{\mathrm{P}}(\mathbf{X}_{k-1},\mathbf{P}_{\mathrm{t},k-1},\mathbf{T}_{\mathrm{d},k-1},\mathbf{W}_{k-1},\boldsymbol{\lambda}_{k-1})\\&+\mathbf{J}_{\mathrm{Z}}(\mathbf{X}_{k|k-1},\mathbf{P}_{\mathrm{t},k},\mathbf{T}_{\mathrm{d},k},\mathbf{W}_k,\boldsymbol{\lambda}_k),\end{aligned}\tag{14}$$

where $\mathbf{X}_{k|k-1}$ denotes the predicted target state vector at the $(k-1)$-th instant. For the sake of convenience, we define the corresponding vectors of the distributed radar network at instant k as $\mathbf{P}_{\mathrm{t},k}$, $\mathbf{T}_{\mathrm{d},k}$, $\mathbf{W}_k$, and $\boldsymbol{\lambda}_k$, to stand for the working parameters corresponding to all the nodes, i.e.:

$$\begin{cases}\mathbf{P}_{\mathrm{t},k}=[P_{\mathrm{t},1,k},P_{\mathrm{t},2,k},\cdots,P_{\mathrm{t},N,k}]^T,\\ \mathbf{T}_{\mathrm{d},k}=[T_{\mathrm{d},1,k},T_{\mathrm{d},2,k},\cdots,T_{\mathrm{d},N,k}]^T,\\ \mathbf{W}_k=[W_{1,k},W_{2,k},\cdots,W_{N,k}]^T,\\ \boldsymbol{\lambda}_k=[\lambda_{1,k},\lambda_{2,k},\cdots,\lambda_{N,k}]^T,\end{cases}\tag{15}$$

where $\mathbf{J}_{\mathrm{P}}(\mathbf{X}_{k-1},\mathbf{P}_{\mathrm{t},k-1},\mathbf{T}_{\mathrm{d},k-1},\mathbf{W}_{k-1},\boldsymbol{\lambda}_{k-1})$ is the prior information BIM, and $\mathbf{J}_{\mathrm{Z}}(\mathbf{X}_{k|k-1},\mathbf{P}_{\mathrm{t},k},\mathbf{T}_{\mathrm{d},k},\mathbf{W}_k,\boldsymbol{\lambda}_k)$ is the measurement BIM. According to the calculations in [27][31], the analytical expression for the predicted BIM can be written as:

$$\begin{aligned}&\mathbf{J}(\mathbf{X}_{k|k-1},\mathbf{P}_{\mathrm{t},k},\mathbf{T}_{\mathrm{d},k},\mathbf{W}_k,\boldsymbol{\lambda}_k)\\&=\sum_{m=1}^{M}\big[\mu_{m,k|k-1}[\mathbf{Q}_{k-1}+\\&\mathbf{F}_m\mathbf{J}^{-1}(\mathbf{X}_{k-1},\mathbf{P}_{\mathrm{t},k-1},\mathbf{T}_{\mathrm{d},k-1},\mathbf{W}_{k-1},\boldsymbol{\lambda}_{k-1})\mathbf{F}_m^T]^{-1}\big]\\&+\sum_{n=1}^{N}\left[\mathbf{H}_{n,k}^T\boldsymbol{\Psi}_{n,k}^{-1}\mathbf{H}_{n,k}\right]\Big|_{\mathbf{X}_{k|k-1}},\end{aligned}\tag{16}$$

where $\mu_{m,k|k-1}$ denotes the predicted probability of model m at instant $(k-1)$, $\mathbf{F}_m$ denotes the state transition matrix of model m with $\mathbf{F}_m\in\{\mathbf{F}_{\mathrm{CV}},\mathbf{F}_{\mathrm{CT}}\}$, and $\mathbf{H}_{n,k}=\left[\nabla_{\mathbf{X}_{k|k-1}}\left(\mathbf{h}_{n,k}(\mathbf{X}_{k|k-1})\right)^T\right]^T$ denotes the Jacobian matrix of the non-linear observation function.

Finally, the predicted BCRLB is defined as the inverse of the predicted BIM in Equation (16):

$$\mathbf{C}_{\mathrm{BCRLB},k}=\left[\mathbf{J}(\mathbf{X}_{k|k-1},\mathbf{P}_{\mathrm{t},k},\mathbf{T}_{\mathrm{d},k},\mathbf{W}_k,\boldsymbol{\lambda}_k)\right]^{-1},\tag{17}$$

where the diagonal elements of the matrix $\mathbf{C}_{\mathrm{BCRLB},k}$ represent the lower bounds on the variances of the predicted estimates of target position and velocity, respectively. Then, to characterize the target tracking accuracy, we utilize the following criterion function:

$$\begin{aligned}&\mathbb{F}(\mathbf{X}_{k|k-1},\mathbf{P}_{\mathrm{t},k},\mathbf{T}_{\mathrm{d},k},\mathbf{W}_k,\boldsymbol{\lambda}_k)\\&\triangleq\sqrt{\mathbf{C}_{\mathrm{BCRLB},k}(1,1)+\mathbf{C}_{\mathrm{BCRLB},k}(2,2)},\end{aligned}\tag{18}$$

where $\mathbf{C}_{\mathrm{BCRLB},k}(1,1)$ and $\mathbf{C}_{\mathrm{BCRLB},k}(2,2)$ represent the first and second elements on the diagonal of the matrix $\mathbf{C}_{\mathrm{BCRLB},k}$, which stand for the lower bounds on the variances of the predicted target positions on the X and Y axes respectively.

C. Performance Metric for Low Probability of Interception

As indicated in [20][32][33], the probability of intercept has been widely employed to evaluate the LPI performance for radar systems. Mathematically speaking, the closed-form expression for probability of intercept is a function of several parameters, such as the transmit power, dwell time, revisit interval, search time of interceptor, and so forth. Previously,

the probability of intercept for the n-th radar node at instant k has already been derived in [20] as follows:

$$p_{\mathrm{I},n,k}(P_{\mathrm{t},n,k},T_{\mathrm{d},n,k}) = \frac{T_{\mathrm{d},n,k}}{2T_{\mathrm{I}}} \times \mathrm{erfc}\left(\sqrt{-\ln p'_{\mathrm{fa}}} - \sqrt{\frac{P_{\mathrm{t},n,k}G_{\mathrm{t},n}G_{\mathrm{I}}\lambda_{\mathrm{t}}^2 G_{\mathrm{IP}}}{(4\pi)^2 R_{n,k}^2 k_0 T_0 B_{\mathrm{I}} F_{\mathrm{I}}} + 0.5}\right), \quad (19)$$

where

$$\mathrm{erfc}(x) = 1 - \frac{2}{\sqrt{\pi}}\int_0^x \exp(-z^2)dz, \quad (20)$$

T_{I} is the search time of intercept receiver, which means the total time required to search all the specified frequency bands and beam positions. In practice, the dwell time is much smaller than the interceptor search time, i.e., $T_{\mathrm{d},n,k} \ll T_{\mathrm{I}}$ [32]. $T_{\mathrm{d},n,k}$ is the dwell time of the n-th radar system at frame k, $P_{\mathrm{t},n,k}$ is the transmit power at instant k, $G_{\mathrm{t},n}$ is the transmitting antenna gain of radar n, G_{I} is the receiving antenna gain of intercept receiver, G_{IP} is the processing gain of intercept receiver, B_{I} is the frequency bandwidth of interceptor, F_{I} is the noise factor of interceptor, and $R_{n,k}$ denotes the distance between the n-th radar node and the target at each frame k. It also needs to be supposed that the frequency search range of intercept receiver is much larger than the waveform bandwidth, namely, $B_{\mathrm{I}} \gg W_{n,k}$.

Since there are multiple active nodes in the distributed phased array radar network, the overall probability of intercept at the k-th frame is defined in the following to gauge the LPI performance of the underlying system:

$$p_{\mathrm{I},k}^{\mathrm{tot}}(\mathbf{P}_{\mathrm{t},k},\mathbf{T}_{\mathrm{d},k}) \triangleq 1 - \prod_{n=1}^{N}\left[1 - p_{\mathrm{I},n,k}(P_{\mathrm{t},n,k},T_{\mathrm{d},n,k})\right]. \quad (21)$$

Here, without loss of generality, it is assumed the corresponding parameters of the hostile intercept receiver, such as search time, receiving antenna gain, processing gain, frequency bandwidth, etc, are known as prior knowledge, which can be acquired according to the military intelligence and information.

Remark 2: Fusing Equations (18) and (21), it is worth pointing out that several working variables have impacts on the proposed JTRMWS scheme. To be specific, not only the illumination resource but also the waveform parameters affect the tracking estimation error, whereas only the transmit power and dwell time are related to the probability of intercept.

D. Mathematical Formulation of the JTRMWS Model

Overall speaking, the purpose of the current study is to simultaneously maximize the target tracking accuracy and LPI performance of distributed phased array radar network by jointly adjusting the transmit power, dwell time, waveform bandwidth, and pulse length of multiple radar nodes, while satisfying some illumination resource budgets and waveform library limitation. Subsequently, the mathematical representation of the optimization problem at each instant k can be described as:

$$\begin{aligned}(\mathcal{P}1)\quad & \min_{\mathbf{P}_{\mathrm{t},k},\mathbf{T}_{\mathrm{d},k},\mathbf{W}_k,\boldsymbol{\lambda}_k} \mathbb{F}(\mathbf{X}_{k|k-1},\mathbf{P}_{\mathrm{t},k},\mathbf{T}_{\mathrm{d},k},\mathbf{W}_k,\boldsymbol{\lambda}_k),\\ & \min_{\mathbf{P}_{\mathrm{t},k},\mathbf{T}_{\mathrm{d},k}} p_{\mathrm{I},k}^{\mathrm{tot}}(\mathbf{P}_{\mathrm{t},k},\mathbf{T}_{\mathrm{d},k}),\\ & \text{s.t.:}\begin{cases} \overline{P_{\min}} \leqslant P_{\mathrm{t},n,k} \leqslant \overline{P_{\max}}, \forall n,\\ \overline{T_{\min}} \leqslant T_{\mathrm{d},n,k} \leqslant \overline{T_{\max}}, \forall n,\\ W_{n,k} \in W_{\mathrm{set}}, \lambda_{n,k} \in \lambda_{\mathrm{set}}, \forall n,\\ \mathrm{SNR}_{n,k|k-1} \geqslant \mathrm{SNR}_{\min}, \forall n, \end{cases}\end{aligned} \quad (22)$$

where $\overline{P_{\min}}$ and $\overline{P_{\max}}$ represent the lower and upper bounds of the transmit power of each radar node, $\overline{T_{\min}}$ and $\overline{T_{\max}}$ represent the minimum and maximum values of the dwell time of each node. W_{set} and λ_{set} denote the corresponding waveform parameter sets, $\mathrm{SNR}_{\min}$ is the predetermined SNR threshold, and $\mathrm{SNR}_{n,k|k-1}$ is the predicted SNR of radar n at instant $(k-1)$, which is written as:

$$\mathrm{SNR}_{n,k|k-1} = \frac{P_{\mathrm{t},n,k}T_{\mathrm{d},n,k}G_{\mathrm{t},n}G_{\mathrm{r},n}\sigma_n\lambda_{\mathrm{t}}^2 G_{\mathrm{RP}}}{(4\pi)^3 T_{\mathrm{r}} R_{n,k|k-1}^4 k_0 T_0 B_{\mathrm{r}} F_{\mathrm{r}}}, \quad (23)$$

where $R_{n,k|k-1}$ denotes the predicted distance between the n-th radar node and the target at instant $(k-1)$.

The first constraint in $(\mathcal{P}1)$ implies that the transmit power of each radar node is bounded by the minimum and maximum values respectively, while the second one states that the dwell time is also bounded by a time budget. The third constraint represents that the waveform parameters can be properly chosen from the predefined sets $W_{\mathrm{set}} = \{W_{1,k}, W_{2,k}, \cdots, W_{N_W,k}\}$ and $\lambda_{\mathrm{set}} = \{\lambda_{1,k}, \lambda_{2,k}, \cdots, \lambda_{N_\lambda,k}\}$, where N_W and N_λ are the corresponding cardinal numbers of the above two sets. In this way, the transmit waveform pair can be obtained in the library $\Omega \triangleq \{(W_{1,k},\lambda_{1,k}),(W_{2,k},\lambda_{1,k}),\cdots,(W_{N_W,k},\lambda_{N_\lambda,k})\}$. The last constraint states that the achievable SNR value should be no less than the specified threshold $\mathrm{SNR}_{\min}$. It is worth to mention that, owing to the impacts of signal radiation attenuation and fluctuating of target RCS, some radar nodes may not be able to detect the target perfectly during target tracking process. Thus, the minimum SNR threshold for target detection is imposed on the optimization problem $(\mathcal{P}1)$. On the other hand, in order to achieve better trade-off between target tracking accuracy and LPI performance, it is assumed that the ranges from the target to multiple radars have no significant difference.

Remark 3: In practical applications, owing to the signal radiation attenuation and fluctuating of target amplitudes, several radar nodes may not be able to detect the target perfectly during the target tracking period. On the other hand, since the multiple radars in the underlying system are independent with each other, a predetermined target detection performance requirement, that is, $\mathrm{SNR}_{\min}$, should be imposed to each radar in $(\mathcal{P}1)$. Moreover, although higher SNR value means more accurate target tracking performance, it also results in more radio frequency resources being emitted, implying much higher risk of interception for the radar network system. In problem $(\mathcal{P}1)$, both the target tracking accuracy and LPI performance of radar network system are considered at the

same time, where it is beneficial to set a given SNR threshold for target tracking at each radar node.

Remark 4: From problem $(\mathcal{P}1)$, one can observe that minimization of the target tracking error and the probability of intercept of radar network system are two conflicting objectives, which must be taken into account in the meantime. Since the optimization model $(\mathcal{P}1)$ is a bi-objective problem, there is a set of Pareto optimal solutions, which satisfy the two different objectives at an acceptable level and are assumed to be equally viable. In addition, it is noted that different Pareto optimal solutions correspond to different balances between target tracking accuracy and LPI performance. Here, the trade-off which can achieve less target tracking error and smaller probability of intercept simultaneously is preferred.

E. Three-Stage-Based Solution Methodology

The optimization model of JTRMWS in $(\mathcal{P}1)$ involves four variables of interest, i.e., the transmit power vector $\mathbf{P}_{\mathrm{t},k}$, the dwell time vector $\mathbf{T}_{\mathrm{d},k}$, the waveform bandwidth vector $\mathbf{W}_k$, and the pulse length vector $\boldsymbol{\lambda}_k$. From the standpoint of mathematics, the proposed JTRMWS strategy is a non-linear and non-convex optimization problem [34]. On the other hand, the above four parameters are all coupled in the objective functions and constraints. As such, it is quite difficult to find the optimal solutions to problem $(\mathcal{P}1)$ directly. In this scenario, an efficient and fast three-stage-based solution algorithm is proposed to deal with the initial non-linear and non-convex optimization problem.

1) Relaxation Reformulation and Problem Partition: Due to the discrete waveform parameter constraints in $(\mathcal{P}1)$, the original optimization formulation is non-convex. Moreover, as previously mentioned, the probability of intercept depends only on the illumination power and dwell time, whereas both the transmit resource and waveform parameters have influence on the target tracking performance [23]. Thus, to solve this kind of problem, a reasonable and intuitive solution is to partition the transmit resource (that is, $\mathbf{P}_{\mathrm{t},k}$, $\mathbf{T}_{\mathrm{d},k}$) and waveform parameters (that is, $\mathbf{W}_k$, $\boldsymbol{\lambda}_k$). Therefore, the initial optimization problem $(\mathcal{P}1)$ is partitioned as:

$$(\mathcal{P}2.1)\quad \min_{\mathbf{P}_{\mathrm{t},k},\mathbf{T}_{\mathrm{d},k}} p_{\mathrm{I},k}^{\mathrm{tot}}(\mathbf{P}_{\mathrm{t},k},\mathbf{T}_{\mathrm{d},k}),\quad \text{s.t.:}\begin{cases}\overline{P_{\min}}\leqslant P_{\mathrm{t},n,k}\leqslant\overline{P_{\max}},\forall n,\\ \overline{T_{\min}}\leqslant T_{\mathrm{d},n,k}\leqslant\overline{T_{\max}},\forall n,\\ \mathrm{SNR}_{n,k|k-1}\geqslant\mathrm{SNR}_{\min},\forall n,\end{cases}\tag{24}$$

and

$$(\mathcal{P}2.2)\quad \min_{\mathbf{P}_{\mathrm{t},k},\mathbf{T}_{\mathrm{d},k},\mathbf{W}_k,\boldsymbol{\lambda}_k} \mathbb{F}(\mathbf{X}_{k|k-1},\mathbf{P}_{\mathrm{t},k},\mathbf{T}_{\mathrm{d},k},\mathbf{W}_k,\boldsymbol{\lambda}_k),\quad \text{s.t.:}\begin{cases}\overline{P_{\min}}\leqslant P_{\mathrm{t},n,k}\leqslant\overline{P_{\max}},\forall n,\\ \overline{T_{\min}}\leqslant T_{\mathrm{d},n,k}\leqslant\overline{T_{\max}},\forall n,\\ W_{n,k}\in W_{\mathrm{set}},\lambda_{n,k}\in\lambda_{\mathrm{set}},\forall n,\\ \mathrm{SNR}_{n,k|k-1}\geqslant\mathrm{SNR}_{\min},\forall n,\end{cases}\tag{25}$$

Furthermore, according to Equations (19) and (21), since the overall probability of intercept of the radar network system depends on the probability of intercept of each node, the sub-problem $(\mathcal{P}2.1)$ can equivalently be reformulated as:

$$(\mathcal{P}2.1.1)\quad \min_{\mathbf{P}_{\mathrm{t},k},\mathbf{T}_{\mathrm{d},k}} p_{\mathrm{I},n,k}(P_{\mathrm{t},n,k},T_{\mathrm{d},n,k}),\quad \text{s.t.:}\begin{cases}\overline{P_{\min}}\leqslant P_{\mathrm{t},n,k}\leqslant\overline{P_{\max}},\forall n,\\ \overline{T_{\min}}\leqslant T_{\mathrm{d},n,k}\leqslant\overline{T_{\max}},\forall n,\\ \mathrm{SNR}_{n,k|k-1}\geqslant\mathrm{SNR}_{\min},\forall n,\end{cases}\tag{26}$$

Hereinafter, by employing the structures of the above two sub-problems $(\mathcal{P}2.1.1)$ and $(\mathcal{P}2.2)$, the corresponding solution methods are developed in the sequel to obtain the sub-optimal solutions in real time.

2) Transmit Resource Management: As implied in [20], the minimum transmit resource consumption of radar system is achieved when the attainable SNR value $\mathrm{SNR}_{n,k|k-1}$ is equal to the specified threshold $\mathrm{SNR}_{\min}$, that is:

$$\frac{P_{\mathrm{t},n,k}T_{\mathrm{d},n,k}G_{\mathrm{t},n}G_{\mathrm{r},n}\sigma_n\lambda_{\mathrm{t}}^2G_{\mathrm{RP}}}{(4\pi)^3T_{\mathrm{r}}R_{n,k|k-1}^4k_0T_0B_{\mathrm{r}}F_{\mathrm{r}}}=\mathrm{SNR}_{\min}.\tag{27}$$

Rearranging the above equation, we can have:

$$P_{\mathrm{t},n,k}=\mathrm{SNR}_{\min}\frac{(4\pi)^3T_{\mathrm{r}}R_{n,k|k-1}^4k_0T_0B_{\mathrm{r}}F_{\mathrm{r}}}{T_{\mathrm{d},n,k}G_{\mathrm{t},n}G_{\mathrm{r},n}\sigma_n\lambda_{\mathrm{t}}^2G_{\mathrm{RP}}}.\tag{28}$$

By substituting Equation (28) into Equation (21), we obtain:

$$p_{\mathrm{I},n,k}(P_{\mathrm{t},n,k},T_{\mathrm{d},n,k})=\frac{T_{\mathrm{d},n,k}}{2T_{\mathrm{I}}}\cdot\mathrm{erfc}\left(\sqrt{-\ln p_{\mathrm{fa}}'}-\sqrt{\frac{4\pi\mathrm{SNR}_{\min,n}T_{\mathrm{r}}B_{\mathrm{r}}F_{\mathrm{r}}G_{\mathrm{I}}G_{\mathrm{IP}}R_{n,k|k-1}^2}{T_{\mathrm{d},n,k}B_{\mathrm{I}}F_{\mathrm{I}}G_{\mathrm{r},n}\sigma_{\mathrm{t}}G_{\mathrm{RP}}}+0.5}\right).\tag{29}$$

With some further mathematical manipulation, it is shown that the probability of intercept of each radar node is a convex upward function with respect to the dwell time. The detailed proof is provided in Appendix A. That is to say, the optimal value of dwell time can be obtained at the boundary of time budget, i.e.:

$$T_{\mathrm{d},n,k}=\arg\min\left[p_{\mathrm{I},n,k}(P_{\mathrm{t},n,k},\overline{T_{\min}}),p_{\mathrm{I},n,k}(P_{\mathrm{t},n,k},\overline{T_{\max}})\right].\tag{30}$$

Equation (30) means that the optimal value of dwell time is either $\overline{T_{\min}}$ or $\overline{T_{\max}}$. As for which one to choose, it depends on which value makes the probability of intercept smaller.

Subsequently, the transmit power of radar node n at instant k can be calculated with Equation (28).

3) Waveform Parameter Selection: After the feasible transmit power and dwell time results $\widehat{\mathbf{P}}_{\mathrm{t},k}$ and $\widehat{\mathbf{T}}_{\mathrm{d},k}$ are acquired, the corresponding variables can be removed in the optimization model $(\mathcal{P}2.2)$. Then, the sub-problem $(\mathcal{P}2.2)$ can be converted to the following form:

$$(\mathcal{P}2.2.1)\quad \min_{\mathbf{W}_k,\boldsymbol{\lambda}_k} \mathbb{F}(\mathbf{X}_{k|k-1},\widehat{\mathbf{P}}_{\mathrm{t},k},\widehat{\mathbf{T}}_{\mathrm{d},k},\mathbf{W}_k,\boldsymbol{\lambda}_k),\quad \text{s.t.:}W_{n,k}\in W_{\mathrm{set}},\lambda_{n,k}\in\lambda_{\mathrm{set}},\forall n.\tag{31}$$

Although the exhaustive search-based or brute force search-based techniques can be exploited to tackle the sub-problem $(\mathcal{P}2.2.1)$, it requires an exponential computational complexity [36]. In this article, we turn to the means of PSO for solving the sub-problem of waveform selection. It is known that,

owing to the quick convergence and easy implementation, the PSO algorithm has been widespread used in engineering practice, which is motivated from the behavior of bird flocking [37]-[39]. During the iteration procedure, each particle, which represents a single solution, adjusts its own position and velocity according to its best previous search experience and the best experience of other neighbors.

In the sub-problem $(\mathcal{P}2.2.1)$, it should be remembered that our goal is to optimize the target tracking accuracy by adaptively selecting the appropriate waveform bandwidth and pulse length of each radar in the waveform library Ω. Intuitively, these waveform parameters are mapped to the positions of the particles, where the position and velocity of the q-th particle are defined as follows:

$$\begin{cases} \mathbf{Y}_q = [W_{q,1,k}, \cdots, W_{q,N,k}, \lambda_{q,1,k}, \cdots, \lambda_{q,N,k}]^T, \\ \mathbf{V}_q = [V^W_{q,1,k}, \cdots, V^W_{q,N,k}, V^\lambda_{q,1,k}, \cdots, V^\lambda_{q,N,k}]^T, \end{cases} \tag{32}$$

where $\mathbf{Y}_q$ and $\mathbf{V}_q$ denote the position and velocity of the q-th particle, respectively. Then, the position and velocity of particle q can be updated as:

$$\begin{cases} \mathbf{Y}_q^{(l+1)} = \mathbf{Y}_q^{(l)} + \mathbf{V}_q^{(l+1)}, \\ \mathbf{V}_q^{(l+1)} = \zeta \mathbf{V}_q^{(l)} + c_1 r_1 \left(\mathbf{P}_q^{(l)} - \mathbf{Y}_q^{(l)} \right) \\ \qquad\quad + c_2 r_2 \left(\mathbf{P}_g^{(l)} - \mathbf{Y}_q^{(l)} \right), \end{cases} \tag{33}$$

where $\mathbf{Y}_q^{(l)}$ and $\mathbf{V}_q^{(l)}$ denote the position and velocity of the q-th particle at iteration l, respectively. ζ denotes the inertia weight, and c_1 and c_2 denote two non-negative constants, which are referred to as acceleration factors. r_1 and r_2 represent the uniformly distributed random numbers between 0 and 1, and l represents the iteration index. $\mathbf{P}_q^{(l)}$ represents the best solution that the q-th particle has obtained until iteration l, and $\mathbf{P}_g^{(l)}$ represents the best solution obtained in the whole population at iteration l [38]. Subsequently, the criterion function shown in Equation (18) is adopted as the fitness function $f\left(\mathbf{Y}_q^{(l)}\right)$ for the sub-problem of waveform selection, where the transmit power and dwell time results have been got in the previous stage. Finally, all the particles are able to converge to the global optimal points through iterative computation and interaction with each other [36]. Note that the position of the global optimal particle represents the selected values of waveform bandwidth and pulse length of all the radar nodes. The detailed steps are summarized in Algorithm 1, according to which we can obtain the best waveform parameters in the available waveform library.

Algorithm 1: The General Steps of the PSO Algorithm for Waveform Selection

Input: Initialize Q particles with position $\mathbf{Y}_q^{(0)}$ and velocity $\mathbf{V}_q^{(0)}$ satisfying the constraint in (31), the inertia weight ζ, the acceleration factors c_1 and c_2, the random numbers r_1 and r_2, the iteration index l, and the maximum iteration number $L_{\max}$.

Output: The global optimal solutions.

repeat
  Calculate the fitness function for $\mathbf{Y}_q^{(l)}$;
  if $f\left(\mathbf{Y}_q^{(l)}\right) < f\left(\mathbf{P}_q^{(l)}\right)$ **then**
    $\mathbf{P}_q^{(l)} \leftarrow \mathbf{Y}_q^{(l)}$;
  end
  if $f\left(\mathbf{Y}_q^{(l)}\right) < f\left(\mathbf{P}_g^{(l)}\right)$ **then**
    $\mathbf{P}_g^{(l)} \leftarrow \mathbf{Y}_q^{(l)}$;
  end
  Update the velocity and position of each particle by using Equation (33);
until $l > L_{max}$ or convergence;
Output the final solutions.

F. Closed-Loop Procedure for the Proposed JTRMWS Scheme

In summary, the proposed JTRMWS scheme employs the feedback information in the target tracking cycle to perform the joint optimization in a distributed phased array radar network. In such a case, we adopt the IMM-EKF technique to obtain the good target state estimate at each tracking instant. After that, the corresponding target information, that is, the predicted BCRLB, is utilized to implement the JTRMWS scheme. In the end, the transmit resource management and waveform selection results are sent back to design the illumination strategy at the next instant, accomplishing the improvements of target tracking accuracy and LPI performance simultaneously.

G. Potential Extension

For the multi-target tracking application, we can utilize the overall target tracking accuracy and LPI performance as the optimization criteria. Then, the resulting optimization model can be established as follows:

$$\begin{aligned} (\mathcal{P}3) \quad & \min_{\mathbf{P}^m_{\mathrm{t},k}, \mathbf{T}^m_{\mathrm{d},k}, \mathbf{W}^m_k, \boldsymbol{\lambda}^m_k} \sum_{m=1}^{M} \mathbb{F}(\mathbf{X}^m_{k|k-1}, \mathbf{P}^m_{\mathrm{t},k}, \mathbf{T}^m_{\mathrm{d},k}, \mathbf{W}^m_k, \boldsymbol{\lambda}^m_k), \\ & \min_{\mathbf{P}^m_{\mathrm{t},k}, \mathbf{T}^m_{\mathrm{d},k}} p^{\mathrm{tot}}_{\mathrm{I},k}(\{\mathbf{P}^m_{\mathrm{t},k}\}_{m=1}^M, \{\mathbf{T}^m_{\mathrm{d},k}\}_{m=1}^M), \\ & \text{s.t.:} \begin{cases} \overline{P_{\min}} \leqslant P^m_{\mathrm{t},n,k} \leqslant \overline{P_{\max}}, \forall n, \\ \sum_{m=1}^M P^m_{\mathrm{t},n,k} \leqslant P_{\mathrm{tot}}, \\ \overline{T_{\min}} \leqslant T^m_{\mathrm{d},n,k} \leqslant \overline{T_{\max}}, \forall n, \\ \sum_{m=1}^M T^m_{\mathrm{d},n,k} \leqslant T_{\mathrm{tot}}, \\ W^m_{n,k} \in W_{\mathrm{set}}, \lambda^m_{n,k} \in \lambda_{\mathrm{set}}, \forall n, \\ \mathrm{SNR}^m_{n,k|k-1} \geqslant \mathrm{SNR}_{\min}, \forall n, \end{cases} \end{aligned} \tag{34}$$

where the overall probability of intercept of the radar network system at the k-th frame $p^{\mathrm{tot}}_{\mathrm{I},k}(\{\mathbf{P}^m_{\mathrm{t},k}\}_{m=1}^M, \{\mathbf{T}^m_{\mathrm{d},k}\}_{m=1}^M)$ is given by:

$$\begin{aligned} & p^{\mathrm{tot}}_{\mathrm{I},k}(\{\mathbf{P}^m_{\mathrm{t},k}\}_{m=1}^M, \{\mathbf{T}^m_{\mathrm{d},k}\}_{m=1}^M) \\ & \triangleq 1 - \prod_{n=1}^{N} \left[1 - p_{\mathrm{I},n,k}\left(\{\mathbf{P}^m_{\mathrm{t},k}\}_{m=1}^M, \{\mathbf{T}^m_{\mathrm{d},k}\}_{m=1}^M\right)\right], \end{aligned} \tag{35}$$

with

$$p_{\mathrm{I},n,k}\left(\{\mathbf{P}_{\mathrm{t},k}^{m}\}_{m=1}^{M},\{\mathbf{T}_{\mathrm{d},k}^{m}\}_{m=1}^{M}\right) = 1-\prod_{m=1}^{M}\left[1-p_{\mathrm{I},n,k}(P_{\mathrm{t},n,k}^{m},T_{\mathrm{d},n,k}^{m})\right], \tag{36}$$

where M is the total number of targets, P_{tot} is the total transmit power of the radar network, T_{tot} is the total dwell time budget, and $\mathrm{SNR}_{n,k|k-1}^{m}$ is the achieved SNR at radar n with respect to target m for the k-th instant. The matrices $\mathbf{P}_{\mathrm{t},k}^{m}$, $\mathbf{T}_{\mathrm{d},k}^{m}$, $\mathbf{W}_{k}^{m}$, and $\boldsymbol{\lambda}_{k}^{m}$ represent the working variables from different radar nodes to target m respectively, that is:

$$\begin{cases}\mathbf{P}_{\mathrm{t},k}^{m}=[P_{\mathrm{t},1,k}^{m},P_{\mathrm{t},2,k}^{m},\cdots,P_{\mathrm{t},N,k}^{m}]^{T},\\ \mathbf{T}_{\mathrm{d},k}^{m}=[T_{\mathrm{d},1,k}^{m},T_{\mathrm{d},2,k}^{m},\cdots,T_{\mathrm{d},N,k}^{m}]^{T},\\ \mathbf{W}_{k}^{m}=[W_{1,k}^{m},W_{2,k}^{m},\cdots,W_{N,k}^{m}]^{T},\\ \boldsymbol{\lambda}_{k}^{m}=[\lambda_{1,k}^{m},\lambda_{2,k}^{m},\cdots,\lambda_{N,k}^{m}]^{T}.\end{cases} \tag{37}$$

Due to the unique characteristics of problem $(\mathcal{P}3)$, the JTRMWS strategy can easily be converted to several sub-problems of single target tracking, which can be resolved independently by the developed three-stage-based methodology. Note that the computational complexity of the JTRMWS strategy in multi-target tracking case would grow larger with the increase of the numbers of targets. To be specific, the computational complexity of the three-stage-based solution technique in such scenario is $\mathcal{O}(MNQL_{\max})$, which is proportional to the number of targets M and the number of radars N. As such, it can be concluded that the joint optimization scheme can straightforwardly be expanded to the multiple targets tracking scenario, which will be addressed in the near future.

IV. Numerical Results and Performance Evaluation

A. Parameter Designation

In this section, several numerical simulation results are provided to demonstrate the effectiveness and superiority of the JTRMWS scheme and analyze the impacts of various factors on the joint optimization results. The distributed phased array radar network with $N = 4$ spatially diverse radar nodes is considered, which aims at minimizing the target tracking error and the probability of intercept of radar network simultaneously employing its available illumination resource. The waveform library Ω consists of 25 waveform types with $\lambda_{\mathrm{set}} = [1,3,5,7,9]\mu$s and $W_{\mathrm{set}} = [0.1,0.3,0.5,0.7,0.9]$MHz. The revisit interval between two successive instants is set to be $\Delta T = 1$ s, and a series of $M_{\mathrm{tot}} = 80$ instants of measurements are exploited to support the numerical simulations. The lower and upper bounds for illumination power of each radar node are $\overline{P_{\mathrm{min}}} = 0$ and $\overline{P_{\mathrm{max}}} = 14$ kW, respectively. The corresponding bounds for dwell time of each node are fixed to be $\overline{T_{\mathrm{min}}} = 5\times10^{-4}$ s and $\overline{T_{\mathrm{max}}} = 2.5\times10^{-2}$ s, respectively. The dwell time is actually known as the coherent accumulation time, which has impact on the coherent accumulation SNR of radar system without affecting the pulse repetition interval. The initial position and velocity of the target are set to be $[60,80]$ km and $[150,260]$ m/s, respectively. The search time of intercept receiver is $T_{\mathrm{I}} = 3$ s. In the PSO method, we set $Q = 20$, $\zeta = 1$, $c_1 = 0.8$, $c_2 = 0.8$, and $L_{\max} = 50$. The other parameters used in the simulations can be found in TABLE I, while the detailed description of the target state is given in TABLE II.

TABLE I
Simulation Parameters

Symbol	Value	Symbol	Value
$G_{\mathrm{t},n}(\forall n)$	36 dB	$G_{\mathrm{r},n}(\forall n)$	35 dB
G_{I}	6 dB	G_{IP}	3 dB
B_{I}	40 GHz	F_{I}	6 dB
G_{RP}	16.5 dB	F_{r}	3 dB
B_{r}	1 MHz	f_{c}	12 GHz
$\mathrm{SNR}_{\mathrm{min}}$	16 dB	$p_{\mathrm{fa}}^{'}$	10^{-8}

TABLE II
The Description of Target Motion

Time slots	Target motion
$1-30$s	Constant velocity
$31-50$s	Right turn($w=3$rad)
$51-80$s	Constant velocity

In the current work, in order to examine the effects of the relative geometry of the radar system with respect to the target, we consider two different simulated scenarios, which are illustrated in Fig. 2. Besides, to better analyze the influence of the target RCS on the joint optimization results, two target reflectivity models are investigated herein. In the first model, it is supposed that the target reflectivity is uniform and its RCS set to be $\sigma_{\mathrm{t}} = 3\mathrm{m}^2$. In the latter one, Fig. 3 depicts the target reflectivities with respect to different radar nodes, respectively. Without loss of generality, it is assumed that the target RCS obeys normal distribution in the second reflectivity model, as shown in Fig. 3, whereas the proposed JTRMWS strategy is also applicable to different target RCS fluctuation models.

B. Case 1: Deployment 1 and Target Reflectivity Model 1

The transmit power and dwell time optimization results of the proposed JTRMWS scheme, obtained from a single Monte-Carlo simulation run, are respectively shown in Fig. 4 and Fig. 5, and the corresponding waveform bandwidth and pulse length selection results are illustrated in Fig. 6 and Fig. 7 respectively, which supports the evaluation of the JTRMWS scheme with the relative geometry of the distributed radar network with respect to the target and the target RCS factored out. From Fig. 5, it can be seen that either the minimum value of dwell time or its maximum value is designated to decrease the probability of intercept of each radar node, which is based on the target motion state in the tracking process and is consistent with the earlier derivations in (27)-(30). It is also worth to mention that the optimization results of the dwell time are varied from one radar to another, which is due to the fact that the multiple radar nodes illuminate the target from various aspect angles. The transmit power of each radar can be calculated according to Equation (28), as depicted in Fig.

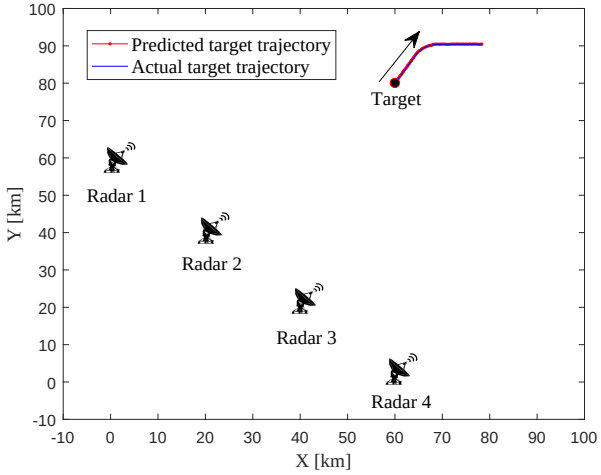

(a)

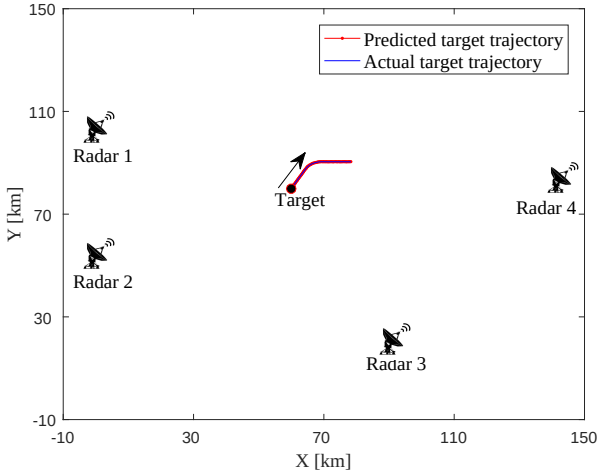

(b)

Fig. 2. Two different deployments of the distributed phased array radar network with respect to the target: (a) Deployment 1; (b) Deployment 2.

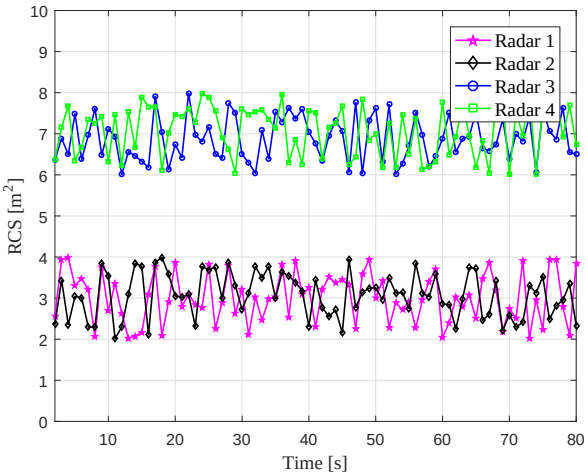

Fig. 3. The second target reflectivity model at each tracking instant.

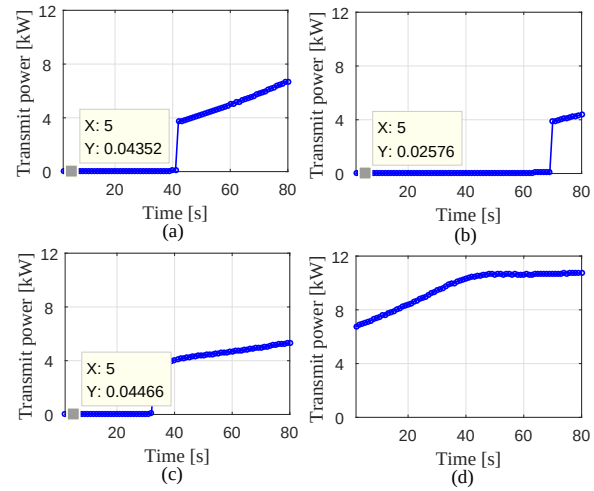

Fig. 4. Transmit power optimization results of the JTRMWS scheme in Case 1: (a) Radar 1; (b) Radar 2; (c) Radar 3; (d) Radar 4.

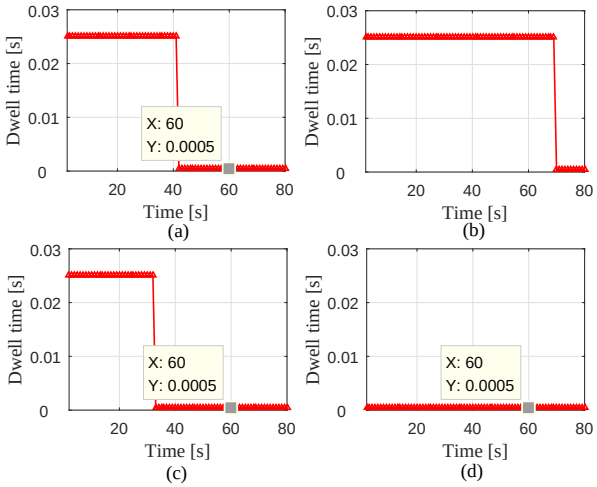

Fig. 5. Dwell time optimization results of the JTRMWS scheme in Case 1: (a) Radar 1; (b) Radar 2; (c) Radar 3; (d) Radar 4.

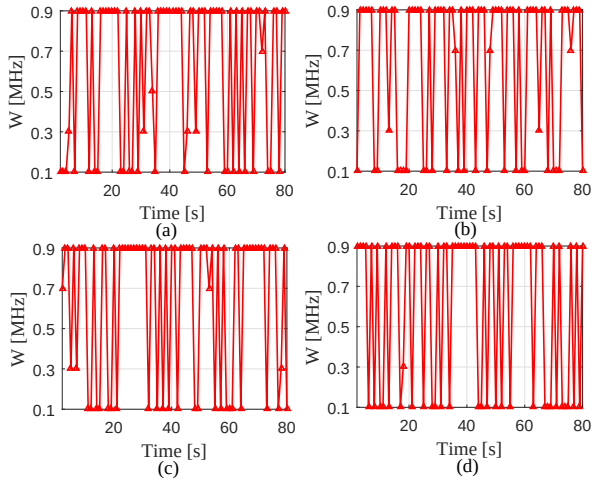

Fig. 6. Waveform bandwidth selection results of the JTRMWS scheme in Case 1: (a) Radar 1; (b) Radar 2; (c) Radar 3; (d) Radar 4.

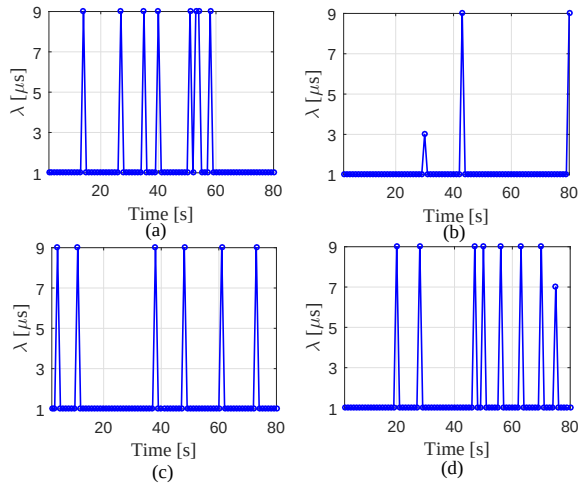

Fig. 7. Waveform pulse length selection results of the JTRMWS scheme in Case 1: (a) Radar 1; (b) Radar 2; (c) Radar 3; (d) Radar 4.

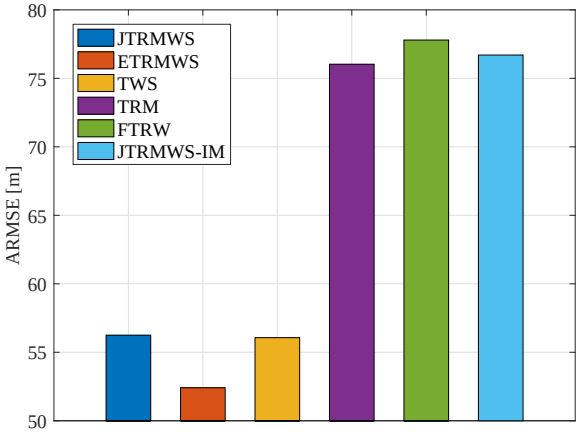

Fig. 8. Comparison of the achievable ARMSE by utilizing different algorithms in Case 1.

4, and it is adaptively optimized to minimize the metric for LPI performance.

Besides, according to Fig. 6 and Fig. 7, the waveform bandwidth and pulse length of each radar node are selected adaptively during the target tracking period. As previously stated, for each radar node, there exists a relationship between transmit waveform parameters, that is, waveform bandwidth and pulse length, and target tracking accuracy. Particularly, the pulse length is related to the range measurement accuracy, while the velocity measurement accuracy is influenced by both waveform bandwidth and pulse length, as shown in Equation (12). As such, combined with the obtained values of illumination power and dwell time, the waveform bandwidth and pulse length are chosen adaptively to optimize the target tracking performance by minimizing the objective function in Equation (18), which are the artifacts of the optimization process.

Furthermore, in order to illustrate the superiorities of the

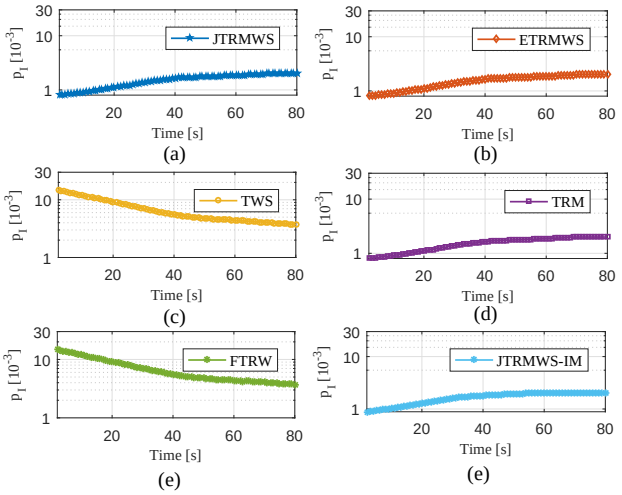

Fig. 9. Comparison of the achievable probability of intercept by utilizing different algorithms in Case 1: (a) JTRMWS; (b) ETRMWS; (c) TWS; (d) TRM; (e) FTRM; (f) JTRMWS-IM.

proposed JTRMWS scheme in terms of target tracking accuracy and LPI performance, its averaged root mean square error (ARMSE) and the corresponding probability of intercept are compared with those of the following four benchmarks in Fig. 8 and Fig. 9 respectively, which is conducted over 150 Monte-Carlo trials:

- Exhaustive transmit resource management and waveform selection (ETRMWS): This algorithm selects the waveform bandwidth and pulse length parameters with an exhaustive search-based approach, while the transmit power and dwell time are optimally designed by solving the optimization model (22).
- Transmit waveform selection (TWS): This algorithm selects the waveform bandwidth and pulse length parameters with the PSO method, while the transmit power and dwell time of each radar node are fixed to be 80W and 2.5×10^{-2}s, respectively.
- Transmit resource management (TRM): The transmit power and dwell time are optimally adjusted by solving the optimization model (22), while the waveform bandwidth and pulse length parameters are fixed to be $W = 0.5$MHz and $\lambda = 5\mu$s, respectively.
- Fixed transmit resource and waveform (FTRW): The transmit power and dwell time are set to be 80W and 2.5×10^{-2}s respectively, while the waveform parameters are set as $W = 0.5$MHz and $\lambda = 5\mu$s, respectively.
- Joint transmit resource management and waveform selection working in independent mode (JTRMWS-IM): This algorithm jointly optimizes the transmit power, dwell time, waveform bandwidth, and pulse length of each radar node, while the multiple radars work in independent mode without collecting and processing the measurements from different nodes.

The tracking ARMSE at instant k is defined at the top of the next page, where M_c represents the total number of Monte-Carlo trials, and $[\hat{x}_{m,k|k}, \hat{y}_{m,k|k}]$ represents the position

estimate of the target at the m-th trial. Note that the achievable ARMSE represents the overall target state estimation accuracy during the whole tracking process. We can observe from those figures that the ETRMWS method is able to achieve the best balance between target tracking accuracy and LPI performance of radar network system, whereas its computational complexity is unacceptable in practice, which will be shown in Section IV-E. It should be pointed out that the proposed JTRMWS scheme aims to get close to the performance of ETRMWS approach. More specifically, although the TWS algorithm has slightly lower target tracking error, the corresponding probability of intercept is much larger than that of the JTRMWS scheme, where the illumination resources are ignored to be optimized to enhance the LPI performance. The reason is that, as aforementioned, both the transmit resources and waveform parameters have influence on the target tracking precision, whereas only the probing power and dwell time affect the LPI performance. On the other side, since there are more degrees of freedom for system optimization, i.e., the transmit power, dwell time, waveform bandwidth, and pulse length variables, the JTRMWS scheme outperforms the TRM and FTRM approaches significantly in terms of the attainable ARMSE and probability of intercept. As for the JTRMWS-IM algorithm, each radar optimizes its transmit resources and waveform parameters independently without collecting and processing the target measurement information from different nodes, resulting in a much worse target tracking error than that of the proposed JTRMWS strategy. Moreover, it is noticeable that the JTRMWS scheme shows very close performance to the ETRMWS algorithm, which confirms the robustness of our developed scheme. To be specific, the attainable ARMSE of the JTRMWS scheme is 7.3% higher than that of the ETRMWS approach, while the values of the achievable probability of intercept of the JTRMWS and ETRMWS algorithms are the same.

In addition, from Fig. 9 (c) and (e), since the transmit power and dwell time of each radar are set to be fixed values in TWS and FTRW methods, the probability of intercept of radar network system only depends on the distances between multiple radar nodes and target. When the target moves away from the radar network, the attainable values of probability of intercept decrease for both TWS and FTRW algorithms. As for JTRMWS, ETRMWS, TRM, and JTRMWS-IM approaches, the probability of intercept of the underlying system is not only a function of the relative distance between radar node and target, but also a function of transmit power and dwell time of each radar. Thus, the corresponding curves exhibit different variation tendencies. In Fig. 9 (f), one can also notice that the achievable probabilities of intercept of the JTRMWS and JTRMWS-IM methods are about the same, whereas the latter one shows worse target tracking performance as illustrated in Fig. 8. Overall, it should be noticed that the proposed JTRMWS scheme is able to not only reduce the target tracking error, but also improve the LPI performance of distributed phased array radar network, validating its advantages over other existing benchmarks.

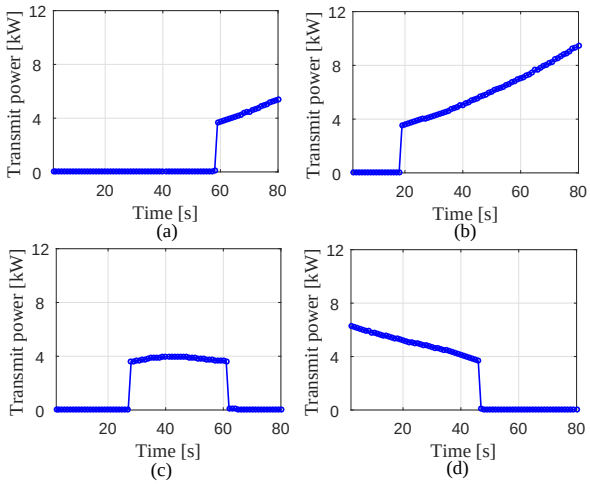

Fig. 10. Transmit power optimization results of the JTRMWS scheme in Case 2: (a) Radar 1; (b) Radar 2; (c) Radar 3; (d) Radar 4.

C. Case 2: Deployment 2 and Target Reflectivity Model 1

In this subsection, we expand the simulation in view of a different deployment of the distributed phased array radar network with respect to the target. The transmit power and dwell time optimization results of the proposed JTRMWS scheme in Case 2 are illustrated in Fig. 10 and Fig. 11 respectively, and the corresponding waveform parameter selection results are given in Fig. 12 and Fig. 13 respectively. It can be seen that, although the above optimization results are quite different from those in Case 1, the same phenomena can also be found in Figs. 10-13, which imply that the transmit resource management and waveform selection results are determined by the relative geometry of the radar network with respect to the moving target.

Fig. 14 and Fig. 15 compare the ARMSE and probability of intercept of the proposed JTRMWS scheme with the other four benchmarks, respectively. Those results further demonstrate that, for the given transmit resource budgets and waveform library, the JTRMWS scheme exhibits very close performance to that of ETRMWS algorithm, which is able to not only improve the tracking precision of the moving target, but also perform enhanced LPI performance of the overall system.

D. Case 3: Deployment 2 and Target Reflectivity Model 2

In this subsection, the impact of the target RCS on the joint optimization results are analyzed. The optimized transmit power and dwell time of each radar node in Case 3 are highlighted in Fig. 16 and Fig. 17 respectively, and the corresponding waveform bandwidth and pulse length selection results are plotted in Fig. 18 and Fig. 19 respectively, which can help us have a deep understanding of the JTRMWS strategy. For the sake of simplicity, it is assumed that the true RCS of the target for the next tracking instant is known as prior information to the radar resource manager. From the above figures, it is apparent that the change of target reflectivity will definitely have significant influence on the transmit resource management and waveform parameter selection results.

$$\text{ARMSE} \triangleq \sqrt{\frac{1}{M_{\text{tot}}}\sum_{k=1}^{M_{\text{tot}}}\frac{1}{M_{\text{c}}}\sum_{m=1}^{M_{\text{c}}}[(x_k-\hat{x}_{m,k|k})^2+(y_k-\hat{y}_{m,k|k})^2]}. \tag{38}$$

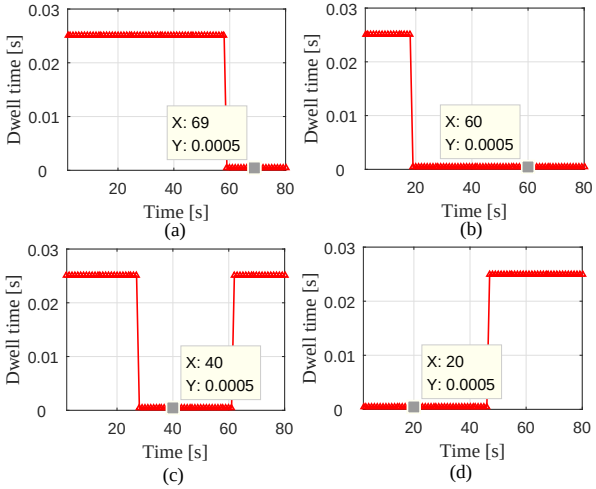

Fig. 11. Dwell time optimization results of the JTRMWS scheme in Case 2: (a) Radar 1; (b) Radar 2; (c) Radar 3; (d) Radar 4.

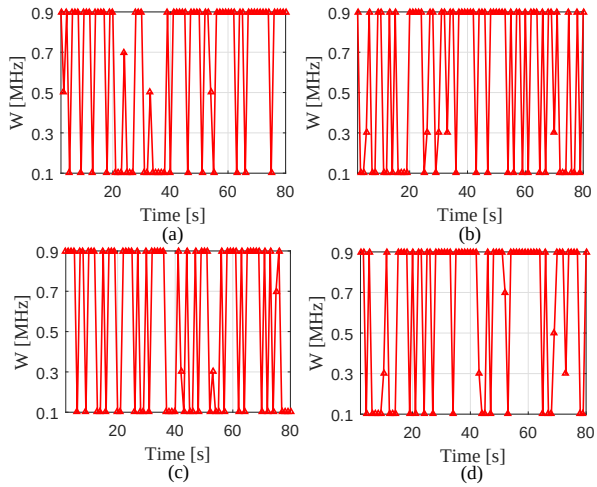

Fig. 12. Waveform bandwith selection results of the JTRMWS scheme: (a) Radar 1; (b) Radar 2; (c) Radar 3; (d) Radar 4.

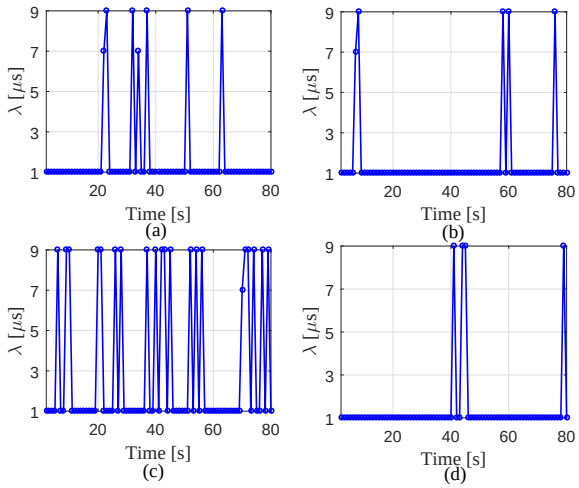

Fig. 13. Waveform pulse length selection results of the JTRMWS scheme in Case 2: (a) Radar 1; (b) Radar 2; (c) Radar 3; (d) Radar 4.

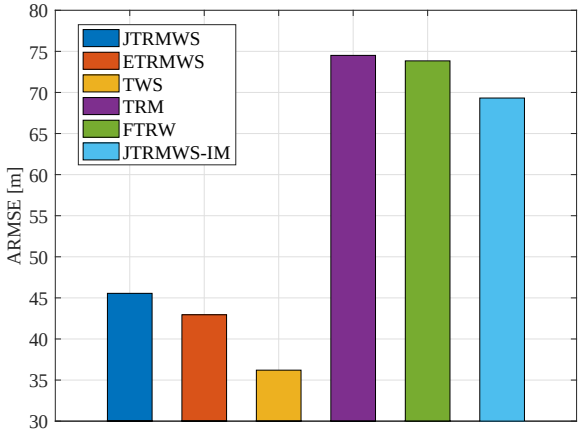

Fig. 14. Comparison of the achievable ARMSE by utilizing different algorithms in Case 2.

For Case 3, the ARMSE and probability of intercept achieved with the JTRMWS scheme are also adopted as the corresponding performance metrics to compare with different benchmarks in Fig. 20 and Fig. 21, respectively. According to these two figures, we can notice that our developed scheme is capable of making better utilization of the available illumination resources of radar network system, and thus can acquire enhanced target tracking accuracy and LPI performance.

E. Computational Complexity Analysis

In Fig. 22, in the cause of demonstrating the timeliness of the developed JTRMWS scheme, its computation time for the full simulation (i.e., 80s) is compared with that of the ETRMWST algorithm in each case. Note that our numerical simulations are carried on a computer with 3.7 MHz CPU and 8 GB RAM running MATLAB 2019a. One can observe that the proposed JTRMWS scheme possesses much lower computational complexity when compared with that of the benchmark, which confirms that the three-stage-based solution approach is efficient in tackling the optimization model and can meet the real-time requirement in practical applications. On the other hand, as shown in previous figures, the differences in terms of the achievable ARMSE and probability of intercept between the above two schemes are quite small,

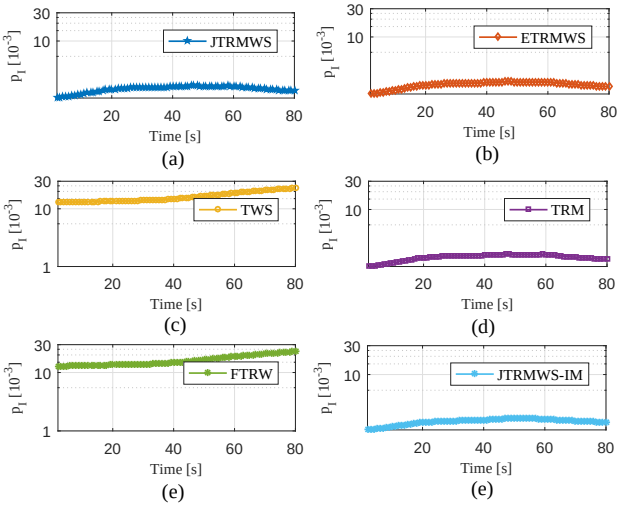

Fig. 15. Comparison of the achievable probability of intercept by utilizing different algorithms in Case 2: (a) JTRMWS; (b) ETRMWS; (c) TWS; (d) TRM; (e) FTRM; (f) JTRMWS-IM.

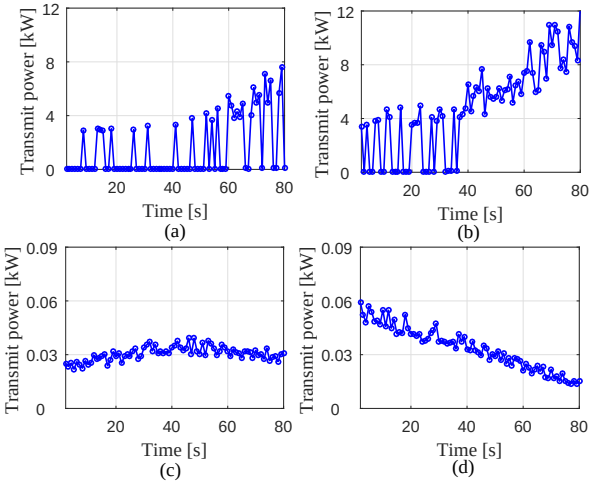

Fig. 16. Transmit power optimization results of the JTRMWS scheme in Case 3:(a) Radar 1; (b) Radar 2; (c) Radar 3; (d) Radar 4.

which further verifies the efficiency and advantages of our presented JTRMWS scheme.

V. Conclusion

In this article, a JTRMWS algorithm is developed for target tracking in a distributed phased array radar network, with the primary objective of enhancing the target tracking accuracy and LPI performance of the underlying system simultaneously by jointly coordinating several working parameters, including the transmit power, dwell time, waveform bandwidth, and pulse length. To facilitate the solving procedure, an efficient and fast three-stage-based solution methodology is put forth to resolve the resulting complex dual-objective and NP-hard optimization problem. Numerical results illustrate that the proposed scheme can efficiently improve the target tracking performance and LPI performance of radar network system.

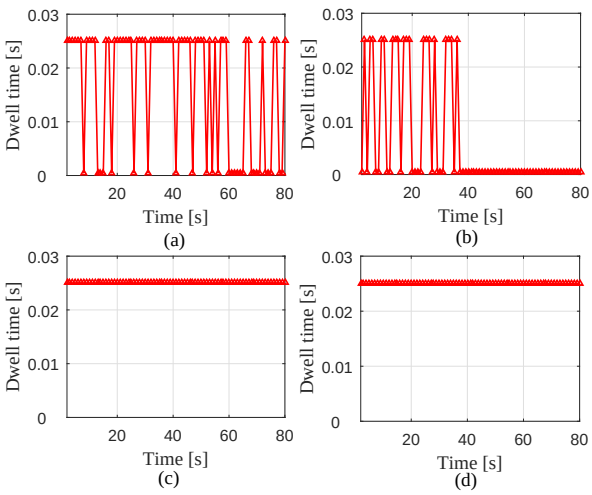

Fig. 17. Dwell time optimization results of the JTRMWS scheme in Case 3:(a) Radar 1; (b) Radar 2; (c) Radar 3; (d) Radar 4.

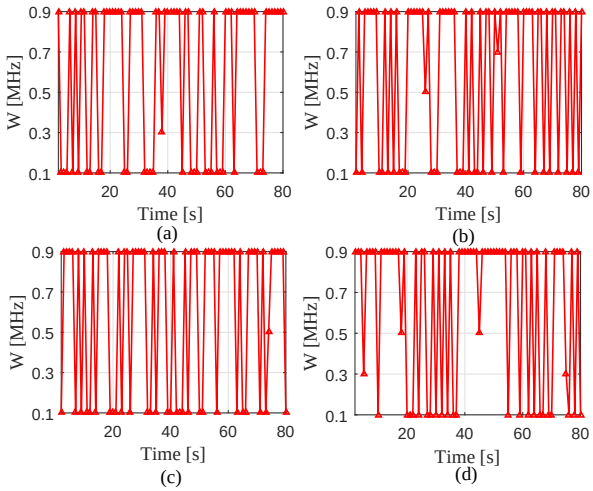

Fig. 18. Waveform bandwidth selection results of the JTRMWS scheme in Case 3:(a) Radar 1; (b) Radar 2; (c) Radar 3; (d) Radar 4.

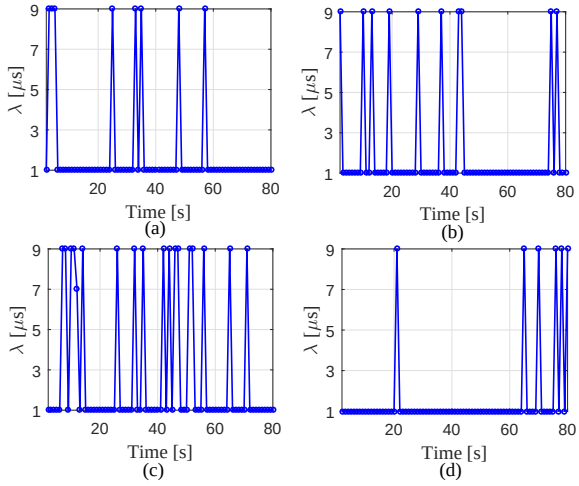

Fig. 19. Waveform pulse length selection results of the JTRMWS scheme in Case 3:(a) Radar 1; (b) Radar 2; (c) Radar 3; (d) Radar 4.

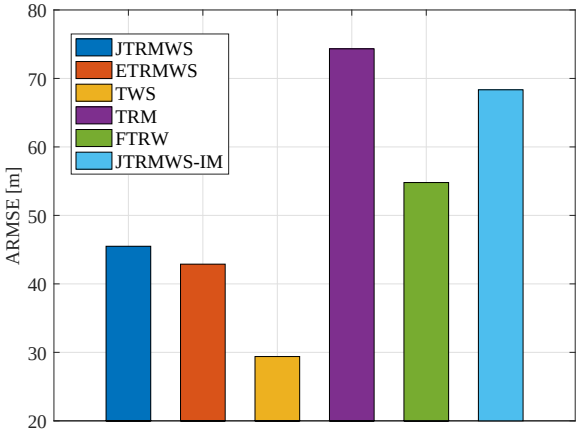

Fig. 20. Comparison of the achievable ARMSE by utilizing different algorithms in Case 3.

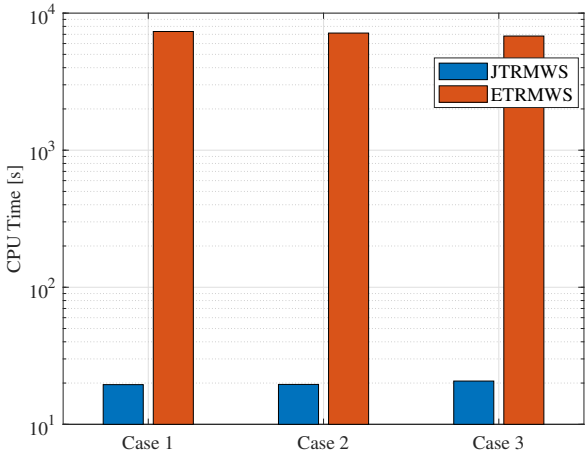

Fig. 22. Comparison of the computation time for the full simulation .

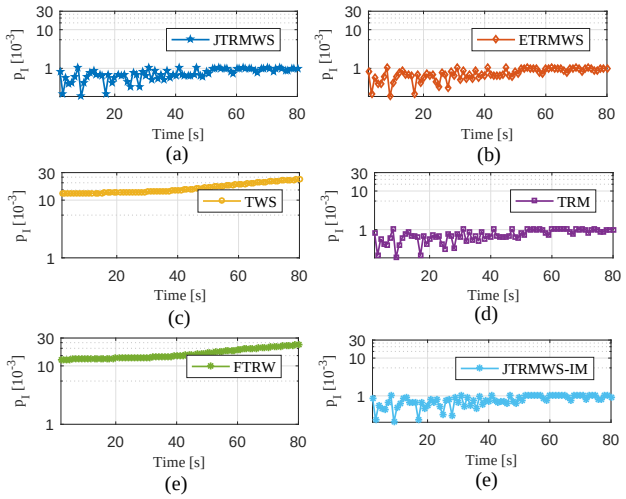

Fig. 21. Comparison of the achievable probability of intercept by utilizing different algorithms in Case 3: (a) JTRMWS; (b) ETRMWS; (c) TWS; (d) TRM; (e) FTRM; (f) JTRMWS-IM.

It is also shown that the proposed JTRMWS strategy can offer unique advantages in terms of tracking accuracy and LPI performance enhancements compared to other existing algorithms. In potential future research, we will take the radar path optimization into account and jointly optimize the available probing resources to further generalize the presented scheme.

APPENDIX A

Let us define $x = T_{\mathrm{d},n,k}$, $a = \sqrt{-\ln p'_{\mathrm{fa}}}$ and $b = \frac{4\pi \mathrm{SNR}_{\min} T_{\mathrm{r}} B_{\mathrm{r}} F_{\mathrm{r}} G_{\mathrm{I}} G_{\mathrm{IP}} R^2_{n,k|k-1}}{B_{\mathrm{I}} F_{\mathrm{I}} G_{r,n} \sigma_{\mathrm{t}} G_{\mathrm{RP}}}$, then Equation (29) can be rewritten as follows:

$$\begin{aligned} p_{\mathrm{I}}(x) &= \frac{x}{2T_{\mathrm{I}}} \cdot \mathrm{erfc}\left(a - \sqrt{\frac{b}{x} + \frac{1}{2}}\right) \\ &= \frac{x}{T_{\mathrm{I}}} \cdot \left(\frac{1}{2} - \frac{1}{\sqrt{\pi}} \int_0^{a-\sqrt{\frac{b}{x}+\frac{1}{2}}} e^{-t^2} dt\right). \end{aligned} \tag{39}$$

First, take the first derivative of $p_{\mathrm{I}}(x)$ with respect to x, we can get:

$$\begin{aligned} \frac{\partial p_{\mathrm{I}}(x)}{\partial x} =& \frac{1}{T_{\mathrm{I}}} \cdot \left(\frac{1}{2} - \frac{1}{\sqrt{\pi}} \int_0^{a-\sqrt{\frac{b}{x}+\frac{1}{2}}} e^{-t^2} dt\right) \\ &+ \frac{1}{4} \frac{e^{-(a-\frac{\sqrt{2}}{2}\sqrt{\frac{2b+x}{x}})^2} \sqrt{2} (\frac{1}{x} - \frac{2b+x}{x^2}) x}{\sqrt{\pi}\sqrt{\frac{2b+x}{x}} T_{\mathrm{I}}}. \end{aligned} \tag{40}$$

Note that the extreme point cannot be obtained by setting $\frac{\partial p_{\mathrm{I}}(x)}{\partial x} = 0$. Thus, take the second derivative of $p_{\mathrm{I}}(x)$ with respect to x, we have the following expression:

$$\begin{aligned} \frac{\partial^2 p_{\mathrm{I}}(x)}{\partial^2 x} =& - b^2 \frac{(\sqrt{2}b + \sqrt{2}xa - \sqrt{x}\sqrt{2b+x})}{T_{\mathrm{I}}(2b+x)^{3/2}\sqrt{\pi}x^{5/2}} \\ & e^{-\frac{1}{4}\frac{(-2ax+\sqrt{2}\sqrt{2b+x}\sqrt{x})^2}{x^2}}. \end{aligned} \tag{41}$$

Here, since the term $-\frac{b^2 e^{-\frac{1}{4}\frac{(-2ax+\sqrt{2}\sqrt{2b+x}\sqrt{x})^2}{x^2}}}{T_{\mathrm{I}}(2b+x)^{3/2}\sqrt{\pi}x^{5/2}} < 0$, it is apparent from Equation (41) that whether $\frac{\partial^2 p_{\mathrm{I}}(x)}{\partial^2 x}$ is positive or not is determined by the function $f(x,a,b) = \sqrt{2}b + \sqrt{2}xa - \sqrt{x}\sqrt{2b+x}$.

Without loss of generality, it is assumed that $f(x,a,b) > 0$. Subsequently, we can obtain:

$$\begin{aligned} &(\sqrt{2}b + \sqrt{2}xa + \sqrt{x}\sqrt{2b+x})(\sqrt{2}b + \sqrt{2}xa - \sqrt{x}\sqrt{2b+x}) \\ &= (2a^2-1)x^2 - (4ab-2b)x + 2b^2 > 0. \end{aligned} \tag{42}$$

It is known that if and only if $\Delta = (4ab-2b)^2 - 8b^2(2a^2-1) \geq 0$, the equation $(2a^2-1)x^2 - (4ab-2b)x + 2b^2 = 0$ has real solutions.

In the current work, since the parameter $a = \sqrt{-\ln p'_{fa}} \in [\sqrt{-\ln 10^{3}}, \sqrt{-\ln 10^{12}}] \approx [2.628, 5.237]$, we have:

$$\Delta = -4b^2(4a-3) < 0. \tag{43}$$

Thus, it can be concluded that the equation $(2a^2-1)x^2 - (4ab-2b)x + 2b^2 = 0$ has no real solutions, and the inequality $(2a^2-1)x^2 - (4ab-2b)x + 2b^2 > 0$ holds all the time. Subsequently, $f(x,a,b) > 0$ holds all the time. That is to say, the second derivative of $p_{\mathrm{I}}(x)$ with respect to x is always less than 0, i.e.:

$$\frac{\partial^2 p_{\mathrm{I}}(x)}{\partial^2 x} < 0. \tag{44}$$

In general, the probability of intercept with respect to dwell time is convex upward.

REFERENCES

[1] A. M. Haimovich, R. S. Blum, and L. J. Cimin. *"MIMO radar with widely separated antennas,"* IEEE Signal Processing Magazine, 2008, 25(1): 116-129.

[2] J. K. Yan, W. Q. Pu, S. H. Zhou, H. W. Liu, and M. S. Greco. *"Optimal resource allocation for asynchronous multiple targets tracking in heterogeneous radar networks,"* IEEE Transactions on Signal Processing, 2020, 68: 4055-4068.

[3] H. Godrich, A. P. Petropulu, and H. V. Poor. *"Power allocation strategies for target localization in distributed multiple-radar architecture,"* IEEE Transactions on Signal Processing, 2011, 59(7): 3226-3240.

[4] C. G. Shi, L. T. Ding, F. Wang, S. Salous, and J. J. Zhou. *"Joint target assignment and resource optimization framework for multitarget tracking in phased array radar network,"* IEEE Systems Journal, 2020, DOI: 10.1109/JSYST.2020.3025867.

[5] H. W. Zhang, B. F. Zong, and J. W. Xie. *"Power and bandwidth allocation for multi-target tracking in collocated MIMO radar,"* IEEE Transactions on Vehicular Technology, 2020, 69(9): 9795-9806.

[6] Y. C. Shi, B. Jiu, J. K. Yan, H. W. Liu, and K. Li. *"Data-driven simultaneous multibeam power allocation: when multiple targets tracking meets deep reinforcement learning,"* IEEE Systems Journal, 2021, 15(1): 1264-1274.

[7] M. C. Xie, W. Yi, T. Kirubarajan, and L. J. Kong. *"Joint node selection and power allocation strategy for multitarget tracking in decentralized radar networks,"* IEEE Transactions on Signal Processing, 2018, 66(3): 729-743.

[8] H. Sun, M. Li, L. Zuo, and R. Q. Cao. *"JPBA of ARN for target tracking in clutter,"* IET Radar Sonar and Navigation, 2019, 13(11): 2024-2033.

[9] W. Yi, Y. Yuan, T. Kirubarajan, and L. J. Kong. *"Resource scheduling for distributed multi-target tracking in netted colocated MIMO radar systems,"* IEEE Transactions on Signal Processing, 2020, 68: 1602-1617.

[10] H. W. Zhang, W. J. Liu, J. W. Xie, Z. J. Zhang, and W. L. Lu. *"Joint subarray selection and power allocation for cognitive target tracking in large-scale MIMO radar networks,"* IEEE Systems Journal, 2020, 14(2): 2569-2580.

[11] Y. Yuan, W. Yi, R. Hoseinnezhad, and P. K. Varshney. *"Robust power allocation for resource-aware multi-target tracking with colocated MIMO radars,"* IEEE Transactions on Signal Processing, 2021, 69: 443-458.

[12] J. K. Yan, J. H. Dai, W. Q. Pu, H. W. Liu, and M. Greco. *"Target capacity based resource optimization for multiple target tracking in radar network,"* IEEE Transactions on Signal Processing, 2021, 69: 2410-2421.

[13] J. K. Yan, W. Q. Pu, S. H. Zhou, H. W. Liu, and Z. Bao. *"Collaborative detection and power allocation framework for target tracking in multiple radar system,"* Information Fusion, 2020, 55: 173-183.

[14] D. E. Lawrence. *"Low probability of intercept antenna array beamforming,"* IEEE Transactions on Antennas and Propagation, 2010, 58(9): 2858-2865.

[15] C. W. Zhou, Y. J. Gu, S. B. He, and Z. G. Shi. *"A robust and efficient algorithm for coprime array adaptive beamforming,"* IEEE Transactions on Vehicular Technology, 2018, 67(2): 1099-1112.

[16] M. A. Govoni, H. B. Li, and J. A. Kosinski. *"Low probability of intercept of an advanced noise radar waveform with linear-FM,"* IEEE Transactions on Aerospace and Electronic Systems, 2013, 49(2): 1351-1356.

[17] C. G. Shi, F. Wang, M. Sellathurai, J. J. Zhou, and S. Salous. *"Low probability of intercept-based optimal power allocation scheme for an integrated multistatic radar and communication system,"* IEEE Systems Journal, 2020, 14(1): 983-994.

[18] C. G. Shi, L. T. Ding, F. Wang, S. Salous, and J. J. Zhou. *"Low probability of intercept-based collaborative power and bandwidth allocation strategy for multi-target tracking in distributed radar network system,"* IEEE Sensors Journal, 2020, 20(12): 6367-6377.

[19] Z. K. Zhang, and Y. B. Tian. *"A novel resource scheduling method of netted radars based on Markov decision process during target tracking in clutter,"* EURASIP Journal on Advances in Signal Processing, 2016, 16, DOI: 10.1186/s13634-016-0309-3.

[20] C. G. Shi, F. Wang, S. Salous and J. J. Zhou. *"Joint transmitter selection and resource management strategy based on low probability of intercept optimization for distributed radar networks,"* Radio Science, 2018, 53(9): 1108-1134.

[21] C. G. Shi, F. Wang, M. Sellathurai, J. J. Zhou, and S. Salous. *"Power minimization-based robust OFDM radar waveform design for radar and communication systems in coexistence,"* IEEE Transactions on Signal Processing, 2018, 66(5): 1316-1330.

[22] Y. X. Lu, Z. S. He, M. L. Deng, and S. L. Liu. *"A cooperative node and waveform allocation scheme in distributed radar network for multiple targets tracking,"* IEEE Radar Conference, 2019: 1-6.

[23] X. Li, T. Cheng, M. Y. Su, and H. Peng. *"Joint time-space resource allocation and waveform selection for the collocated MIMO radar in multiple targets tracking,"* Signal Processing, 2020, 176, DOI: 10.1016/j.sigpro.2020.107650.

[24] W. D. Blair, and Y. Bar-Shalom. *"Multitarget-multisensor tracking: applications and advances,"* Artech House, 2000.

[25] D. J. Kershaw, and R. J. Evans. *"Optimal waveform selection for tracking systems,"* IEEE Transactions on Information Theory, 1994, 40(5): 1536-1550.

[26] N. H. Nguyen, K. Dogancay, and L. M. Davis. *"Adaptive waveform selection for multistatic target tracking,* IEEE Transactions on Aerospace and Electronic Systems, 2015, 51(1): 688701.

[27] J. K. Yan, H. W. Liu, W. Q. Pu, S. H. Zhou, Z. Liu, and Z. Bao. *"Joint beam selection and power allocation for multiple target tracking in netted colocated MIMO radar system,* IEEE Transactions on Signal Processing, 2016, 64(24): 64176427.

[28] M. C. Xie, W. Yi, L. J. Kong, and T. Kirubarajan. *"Receive-beam resource allocation for multiple target tracking with distributed MIMO radars,* IEEE Transactions on Aerospace and Electronic Systems, 2018, 54(5): 24212436.

[29] P. Chavali and A. Nehorai. *"Scheduling and power allocation in a cognitive radar network for multiple-target tracking,* IEEE Transactions on Signal Processing, 2011, 60(2): 715729.

[30] P. Tichavsky, C. H. Muravchik, and A. Nehorai. *"Posterior Cramer-Rao bounds for discrete-time nonlinear filtering,* IEEE Transactions on Signal Processing, 1998, 46(5): 13861396.

[31] H. L. Van Trees, K. L. Bell, and Y. G. Wang. *"Bayesian Cramer-Rao bounds for multistatic radar,"* International Waveform Diversity & Design Conference, 2006: 856-859.

[32] D. Lynch Jr. *"Introduction to RF stealth,* North California: Sci Tech Publishing Inc, 2004.

[33] Y. J. Wang, C. G. Shi, F. Wang, and J. J. Zhou. *"Collaborative transmit resource scheduling and waveform selection for target tracking in multistatic radar system,* IET Radar, Sonar and Navigation, 2021, 15: 209-225.

[34] S. Boyd, and L. Vandenberghe. *"Convex Optimization,"* Cambridge, U.K.: Cambridge University Press, 2004.

[35] N. H. Nguyen, K. Dogancay, and L. M. Davis. *"Adaptive waveform selection for multistatic target tracking,* IEEE Transactions on Aerospace and Electronic Systems, 2015, 51(1): 688701.

[36] H. W. Zhang, J. W. Xie, J. P. Zhang, Z. J. Zhang, and X. L. Fu. *"Sensor scheduling and resource allocation in distributed MIMO radar for joint target tracking and detection,"* IEEE Access, 2019, 7: 62387-62400.

[37] S. Scott-Hayward, and E. Garcia-Palacios. *"Channel time allocation PSO for gigabit multimedia wireless networks,"* IEEE Transactions on Multimedia, 2014, 16(3): 828-836.

[38] A. P. Shrestha, and S. Yoo. *"Optimal Resource Allocation Using Support Vector Machine for Wireless Power Transfer in Cognitive Radio Networks,"* IEEE Transactions on Vehicular Technology, 2018, 67(9): 8525-8535.

[39] W. Li, J. Lei, T. Wang, C. L. Xiong, and J. B. Wei. *"Dynamic optimization for resource allocation in relay-aided OFDMA systems under multiservice,"* IEEE Transactions on Vehicular Technology, 2016, 65(3): 1303-1313.